NaJAZh Regulates a Subset of Defense Responses against Herbivores and Spontaneous Leaf Necrosis in *Nicotiana attenuata* Plants[C][W][OA]

Youngjoo Oh, Ian T. Baldwin, and Ivan Gális[1]*

Department of Molecular Ecology, Max Planck Institute for Chemical Ecology, Jena D–07745, Germany

The JASMONATE ZIM DOMAIN (JAZ) proteins function as negative regulators of jasmonic acid signaling in plants. We cloned 12 *JAZ* genes from native tobacco (*Nicotiana attenuata*), including nine novel *JAZ*s in tobacco, and examined their expression in plants that had leaves elicited by wounding or simulated herbivory. Most *JAZ* genes showed strong expression in the elicited leaves, but *NaJAZg* was mainly expressed in roots. Another novel herbivory-elicited gene, *NaJAZh*, was analyzed in detail. RNA interference suppression of this gene in inverted-repeat (ir)JAZh plants deregulated a specific branch of jasmonic acid-dependent direct and indirect defenses: irJAZh plants showed greater trypsin protease inhibitor activity, 17-hydroxygeranyllinalool diterpene glycosides accumulation, and emission of volatile organic compounds from leaves. Silencing of *NaJAZh* also revealed a novel cross talk in JAZ-regulated secondary metabolism, as irJAZh plants had significantly reduced nicotine levels. In addition, irJAZh spontaneously developed leaf necrosis during the transition to flowering. Because the lesions closely correlated with the elevated expression of programmed cell death genes and the accumulations of salicylic acid and hydrogen peroxide in the leaves, we propose a novel role of the NaJAZh protein as a repressor of necrosis and/or programmed cell death during plant development.

Jasmonic acid (JA) is an important plant signal that regulates the defense of plants against biotic stress. In addition, JA exerts control functions in plant development, such as root growth, senescence, pollen and flower development, tuber formation, and tendril coiling (for review, see Wasternack, 2007). JA rapidly accumulates in mechanically wounded tissues, after attack by herbivores or after infection of plants by necrotrophic pathogens (Farmer et al., 2003; Glazebrook, 2005; Browse and Howe, 2008; Glauser et al., 2008; Howe and Jander, 2008; Wu and Baldwin, 2010). It is produced from membrane lipids in a well-characterized octadecanoid pathway compartmentalized in two plant organelles, chloroplasts and peroxisomes (for review, see Schaller and Stintzi, 2009).

In response to JA, plants accumulate a variety of defense metabolites that reflect the extreme chemical diversity of terrestrial plants. For example, Arabidopsis (*Arabidopsis thaliana*) plants use glucosinolates (amino acid derivatives) for defense (Rask et al., 2000; Mewis et al., 2006; Shroff et al., 2008), whereas tobacco (*Nicotiana* spp.) plants produce nicotinic alkaloids to ward off attack from feeding herbivores (Baldwin et al., 1997; Wink and Roberts, 1998; Shoji et al., 2000; Steppuhn et al., 2004). In addition, most plants produce protease inhibitors in response to herbivory, which inhibit proteolysis and negatively affect the digestibility of ingested plant material in insect guts (Jongsma et al., 1994, 1995; Koiwa et al., 1997; Zavala et al., 2004a; Habib and Fazili, 2007; Hartl et al., 2010). Green leaf volatiles (GLVs) and volatile organic compounds (VOCs) constitute another important plant defense mechanism to attract predators of herbivores; this strategy is also known as indirect plant defense (Halitschke et al., 2000; Kessler and Baldwin, 2001; Baldwin et al., 2002; Allmann and Baldwin, 2010).

Despite the large diversity found in downstream JA-regulated defense responses, the main components of the JA signaling pathway are conserved between plant species. A central component in JA signaling is the CORONATINE INSENSITIVE1 (COI1) protein that was found and functionally analyzed in several plant species (Feys et al., 1994; Xie et al., 1998; Devoto et al., 2002, 2005; Li et al., 2004; Paschold et al., 2008). The F-box protein COI1, as part of the JA receptor complex, contributes to the binding of a bioactive JA derivative, (+)-7-iso-jasmonoyl-L-isoleucine (JA-Ile; Thines et al., 2007; Katsir et al., 2008; Fonseca et al., 2009). In the presence of JA-Ile, COI1 interacts with JASMONATE ZIM DOMAIN (JAZ) repressors that are subsequently ubiquitinated and degraded by the 26S proteasome (Chini et al., 2007; Thines et al., 2007; Yan et al., 2007).

[1] Present address: Institute of Plant Science and Resources, Okayama University, Kurashiki 710–0046, Japan.

* Corresponding author; e-mail igalis@ice.mpg.de.

The author responsible for distribution of materials integral to the findings presented in this article in accordance with the policy described in the Instructions for Authors (www.plantphysiol.org) is: Ian T. Baldwin (baldwin@ice.mpg.de).

[C] Some figures in this article are displayed in color online but in black and white in the print edition.

[W] The online version of this article contains Web-only data.

[OA] Open Access articles can be viewed online without a subscription.

www.plantphysiol.org/cgi/doi/10.1104/pp.112.193771

Because the Jas domain in JAZ is known to bind MYC2-class transcription factors (TFs) that control the expression of a majority of JA-inducible genes (Boter et al., 2004; Lorenzo et al., 2004; Chini et al., 2007; Cheng et al., 2011, Fernández-Calvo et al., 2011; Niu et al., 2011; Shoji and Hashimoto, 2011; Zhang et al., 2012), the degradation of JAZ repressors by the SCF^{COI1} complex leads to the active transcriptional status of JA-dependent genes. In contrast, the accumulation of JAZ proteins, which interact with an EAR domain-containing NINJA protein, represses JA-mediated responses, as EAR binds a strong plant transcriptional corepressor protein, TOPLESS (Pauwels et al., 2010).

The transcriptional activity of MYC2 and MYC2-like TFs, and several additional JA-regulated TFs, therefore, depends on their release from JAZ-imposed repression. The JAZ proteins, typically present as protein families in plants, contain two important functional domains, ZIM and Jas (for review, see Pauwels and Goossens, 2011). The ZIM domain (Shikata et al., 2004; Vanholme et al., 2007) with the TIF[F/Y]XG motif (or its variant), located in the N-terminal part of JAZ proteins, mediates the homomeric and heteromeric interactions between JAZ proteins (Chini et al., 2009; Chung and Howe, 2009) and the binding of the NINJA protein, a strong interactor of the TOPLESS corepressor mentioned above (Pauwels et al., 2010). The Jas domain (Yan et al., 2007) is required for the JAZ/COI1 interaction and the binding of MYC2 TFs. It is characterized by an S-L-X(2)-F-X(2)-K-R-X(2)-R core, delimited by a conserved N-terminal Pro and a C-terminal PY sequence. Two positively charged amino acid residues, Ala-205 and Ala-206, in the Jas domain of the AtJAZ1 protein were shown to be essential for the JAZ/COI1 interaction (Melotto et al., 2008).

Recently, it has been reported that Arabidopsis AtJAZ8 lacks a typical degradation sequence (degron) in its Jas motif that is required for the sealing of JA-Ile in the binding pocket at the COI1-JAZ interface (Sheard et al., 2010; Shyu et al., 2012). In contrast, AtJAZ8 contained an EAR sequence at the N terminus, suggesting that AtJAZ8 may be directly binding the TOPLESS corepressor and repressing TFs without the help of NINJA adaptor proteins (Shyu et al., 2012).

Since the identification of JAZ proteins, much effort has focused on the functional characterization of JAZ complexes, such as the binding of JA-Ile in the coreceptor structure (Melotto et al., 2008; Yan et al., 2009; Sheard et al., 2010), interactions among and splicing of individual JAZ proteins (Chini et al., 2009; Chung et al., 2009, 2010), and interaction of JAZs with various TFs in plants (for review, see Pauwels and Goossens, 2011). To demonstrate the regulatory function of JAZ proteins, Jas-truncated or alternatively spliced forms of JAZ proteins were efficiently used (Chini et al., 2007; Thines et al., 2007; Shoji et al., 2008; Chung et al., 2010). Such proteins may interfere with the degradation of other JAZ proteins, as previously shown for the *jai3-1* mutant using in vitro degradation assays (Chini et al., 2007), thus causing the wide-ranging dominant JA-insensitive phenotypes observed in transgenic or mutant plants, including male sterility and resistance to JA in root growth bioassays.

Despite current progress in the general understanding of JAZ proteins as repressors of JA signaling, the functions of individual JAZ proteins in plants remain largely unknown (see final section in Pauwels and Goossens, 2011). To extend the current JAZ repertoire in plants, we cloned 12 full-length *JAZ* genes from native tobacco (*Nicotiana attenuata*) and subsequently initiated a functional screen of JAZ proteins in this ecologically relevant plant model. Here, we show that silencing the *NaJAZh* gene results in a dramatic shift in the regulation of JA-dependent responses in *N. attenuata*. In addition, the NaJAZh-deficient plants developed spontaneous necrotic lesions on the leaves, a novel phenotype associated with JA signaling in plants.

RESULTS

Identification of Novel *N. attenuata* JAZ Proteins

We identified 12 JAZ proteins in *N. attenuata* based on the assembly of tobacco JAZ sequences available in public EST databases, focusing on the presence of characteristic conserved domains, ZIM and Jas, in these proteins. Primers flanking the coding regions of putatively assembled tobacco *JAZ* genes (Supplemental Table S3) were then used in PCR with leaf- and/or root-derived cDNAs from *N. attenuata*. The obtained PCR-amplified fragments were cloned and sequenced to yield 12 distinct *N. attenuata JAZ* genes named *NaJAZa*, *-b*, *-c*, *-d*, *-e*, *-f*, *-g*, *-h*, *-j*, *-k*, *-l*, and *-m* (which include nine novel *JAZ* genes in tobacco). In two cases, we retrieved cDNA clones of variable length that most likely belonged to the same *JAZ* gene (*NaJAZc.1*/*NaJAZc.2* and *NaJAZk.1*/*NaJAZk.2*; Supplemental Fig. S1), suggesting that alternative splicing may occur in the processing of specific *N. attenuata* JAZ transcripts.

When we performed a phylogenetic analysis of full-length NaJAZ proteins, together with JAZ proteins from Arabidopsis (AtJAZ1 to -12; Chung et al., 2008), tomato (*Solanum lycopersicum*; SlJAZ1 to -12; Sun et al., 2011), rice (*Oryza sativa*; OsJAZ1 to -12; Seo et al., 2011), and three already identified JAZ proteins from *Nicotiana tabacum* (NtJAZ1 to -3; Shoji et al., 2008), JAZ proteins clustered into five main subgroups (I–V; Fig. 1; Supplemental Text S1). Four of those contained the members from all plant species (I, III, IV, and V), whereas branch II did not contain any sequence from the monocot rice.

NaJAZ Genes Are Differentially Expressed in Shoot and Root Tissues

Using a previously reported microarray data set (Kim et al., 2011), the expression of 10 individual *N. attenuata JAZ* genes was examined. The rosette leaves of *N. attenuata* plants were untreated, elicited with wounding (punctured with a fabric pattern wheel and

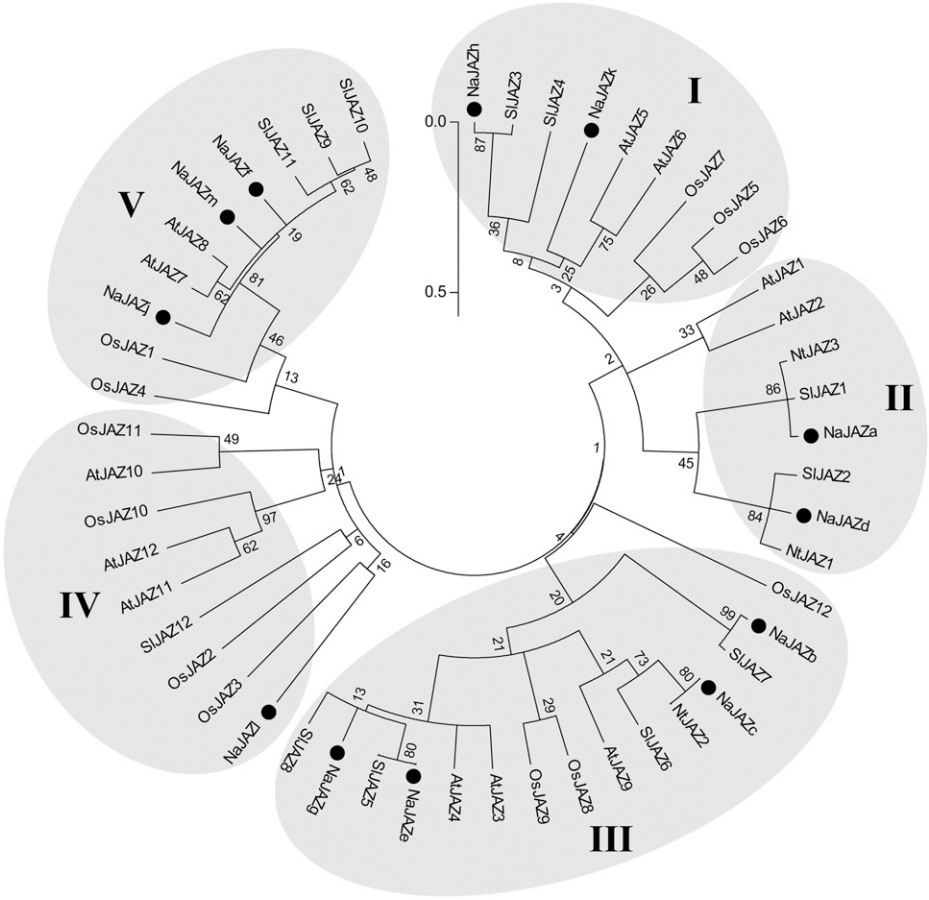

Figure 1. Phylogenetic tree of tobacco, rice, tomato, and Arabidopsis JAZ proteins. The phylogenetic tree was constructed using previously reported tobacco, rice, tomato, and Arabidopsis JAZ proteins and 12 JAZ protein sequences from *N. attenuata* identified in this paper. Protein sequences were aligned with ClustalW, Gonnet matrix gap penalty of 10, and extension penalty of 0.2. The phylogenetic tree was constructed from the alignment using MEGA 5.05 software using the maximum likelihood bootstrap method (1,000 replicates). Black circles indicate the positions of *N. attenuata* proteins in the phylogram.

supplied with water [W+W]), or treated with simulated herbivory (wounds treated with diluted oral secretions from *Manduca sexta* larvae [W+OS]). In addition to expression in the elicited leaf, we also examined expression in the young untreated leaves and roots to monitor systemic induction of *JAZ* genes. As shown in Figure 2, *NaJAZc*, *NaJAZe*, and *NaJAZk* genes were similarly expressed in the leaf and root tissues. In contrast, *NaJAZa*, *NaJAZb*, *NaJAZd*, *NaJAZf*, *NaJAZh*, and *NaJAZj* genes were strongly induced by wounding in the leaves but showed very limited expression in the roots (note the variable *y* axis scales in the graphs in Fig. 2). *NaJAZg* was mainly expressed in roots, showing very low and noninducible expression in leaves. Furthermore, some *N. attenuata JAZ* genes differed in their response to W+W and W+OS treatments. Whereas most *JAZ* genes were highly up-regulated by W+OS treatment in locally elicited and systemic leaves, *NaJAZc* was expressed constitutively across all conditions. Interestingly, *NaJAZe* was more induced by W+W compared with W+OS in the local leaves 1 h after elicitation, suggesting that elicitors in the oral secretion may have suppressed the wound-induced expression of this gene. These differential patterns of expression directly support the previously proposed functional specialization of *JAZ* genes in the defense and growth of plants (Howe and Jander, 2008).

Silencing of NaJAZh Alters the Expression of Other *JAZ* Genes

A subgroup I *NaJAZh* gene (Fig. 1) with transcripts strongly accumulated in response to W+OS in local and systemic leaves (Fig. 2) was selected for detailed functional analysis. This phylogenetic subgroup also contained Arabidopsis *AtJAZ5/6* genes, suggesting a possibly conserved function of these proteins. We transformed *N. attenuata* plants with the inverted-repeat (ir) RNA interference construct of NaJAZh (Supplemental Fig. S2) and suppressed its expression in planta. Three efficiently silenced lines (90%–95% reduction of transcripts in W+OS-elicited plants; Fig. 3A) that contained a single T-DNA insert (Supplemental Fig. S3) were selected for the functional analysis conducted in this paper (irJAZh-264, -267, and -368).

The expression of 11 *NaJAZ* genes was examined in control (untreated) and 1-h W+OS-elicited leaves of irJAZh plants by quantitative PCR (qPCR; Fig. 3B). *NaJAZg*, which could not be reliably detected by qPCR in the leaves, was analyzed together with *NaJAZh* in the roots of rosette leaf W+OS-induced plants (Fig. 3C). In addition to the strongly reduced accumulation of *NaJAZh* transcripts in both root and leaf tissues of irJAZh plants, compared with identically treated tissues of wild-type plants, we found a higher expression

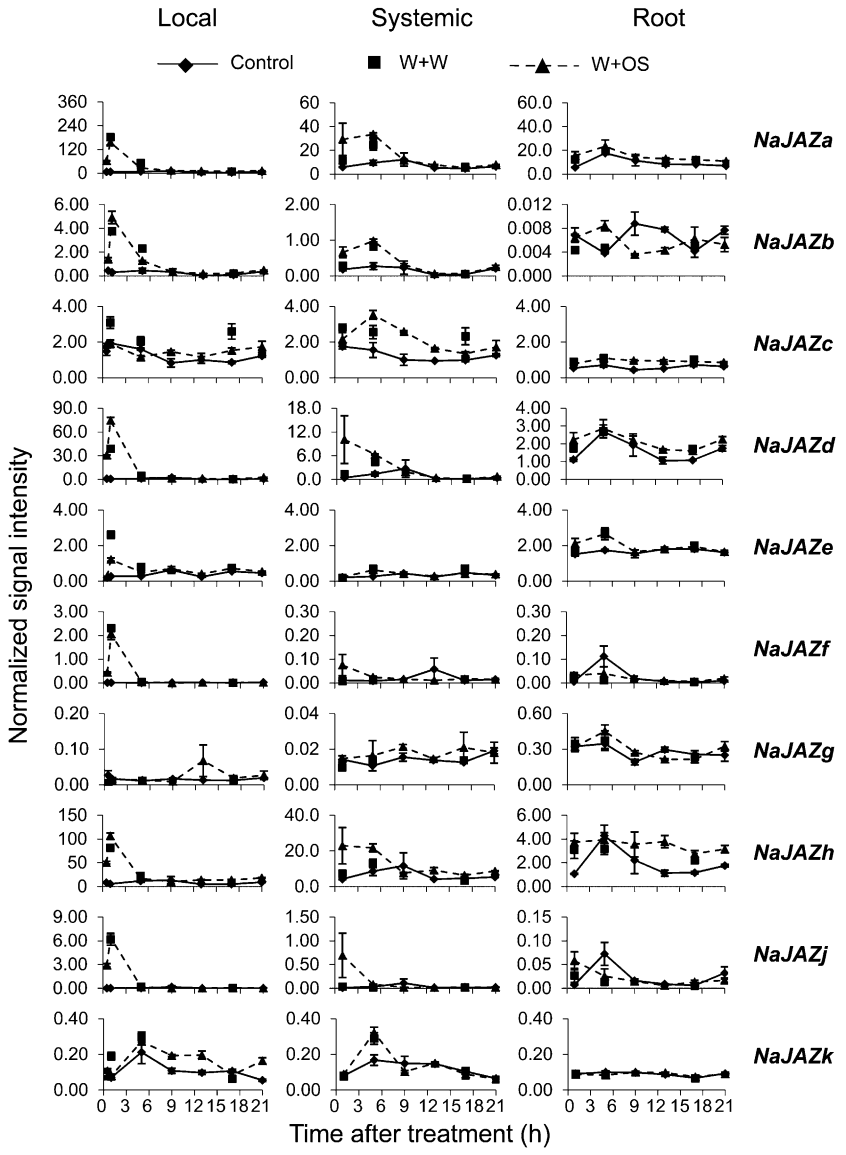

Figure 2. Basal and induced expression of individual *JAZ* genes in *N. attenuata*. The accumulation of *NaJAZ* transcripts in local treated leaves, systemic leaves, and roots was determined by microarrays ($n = 3$) after elicitation of the leaves with wounding (W+W) or simulated herbivory (W+OS); control plants remained untreated. Control and W+OS samples were harvested at 0, 1, 5, 9, 12, 17, and 21 h post elicitation; because samples from the W+W treatment were collected only at 0, 1, 5, and 17 h post elicitation, the time points of the W+W treatments are not connected with lines in the graphs.

of *NaJAZf* (approximately 2-fold) and moderately reduced expression of two additional genes, *NaJAZe* (approximately 1.8-fold) and *NaJAZm* (approximately 2-fold), in irJAZh tissues. However, the NaJAZh silencing construct did not share any obvious similarity with *NaJAZe* and *NaJAZm* genes, and there was no continuous sequence homology of 21 nucleotides (or longer) between *NaJAZe*, *NaJAZm*, and our inverted repeat construct (Supplemental Text S2) that would suggest the possibility of a cosilencing effect. In addition, the increased expression of *NaJAZf* could not be explained by cosilencing mechanisms. The expression of this gene 2 h after oral secretion elicitation of leaves, analyzed in an independent microarray experiment, was approximately five times higher in irJAZh compared with wild-type leaves (Supplemental Fig. S4). The reduction in *NaJAZe* transcripts was not observed in this experiment, possibly due to the analysis of plants at a later time point after elicitation (2 h) relative to the qPCR experiment (1 h; Fig. 3B). The *NaJAZm* probe was not on the microarray chip, and data for this gene could not be compared. Overall, consistent changes in *NaJAZf* expression in irJAZh plants support the existence of a mutual regulatory network among individual JAZ repressors in JA signaling, which is further supported by the presence of G-boxes that bind the MYC2 TF in promoter regions of most Arabidopsis *JAZ* genes (Chini et al., 2007).

NaJAZh Silencing Suppressed the Performance of a Specialist Herbivore without Changing JA-Ile Levels

To examine if W+OS-responsive NaJAZh could regulate defense against herbivores, we performed

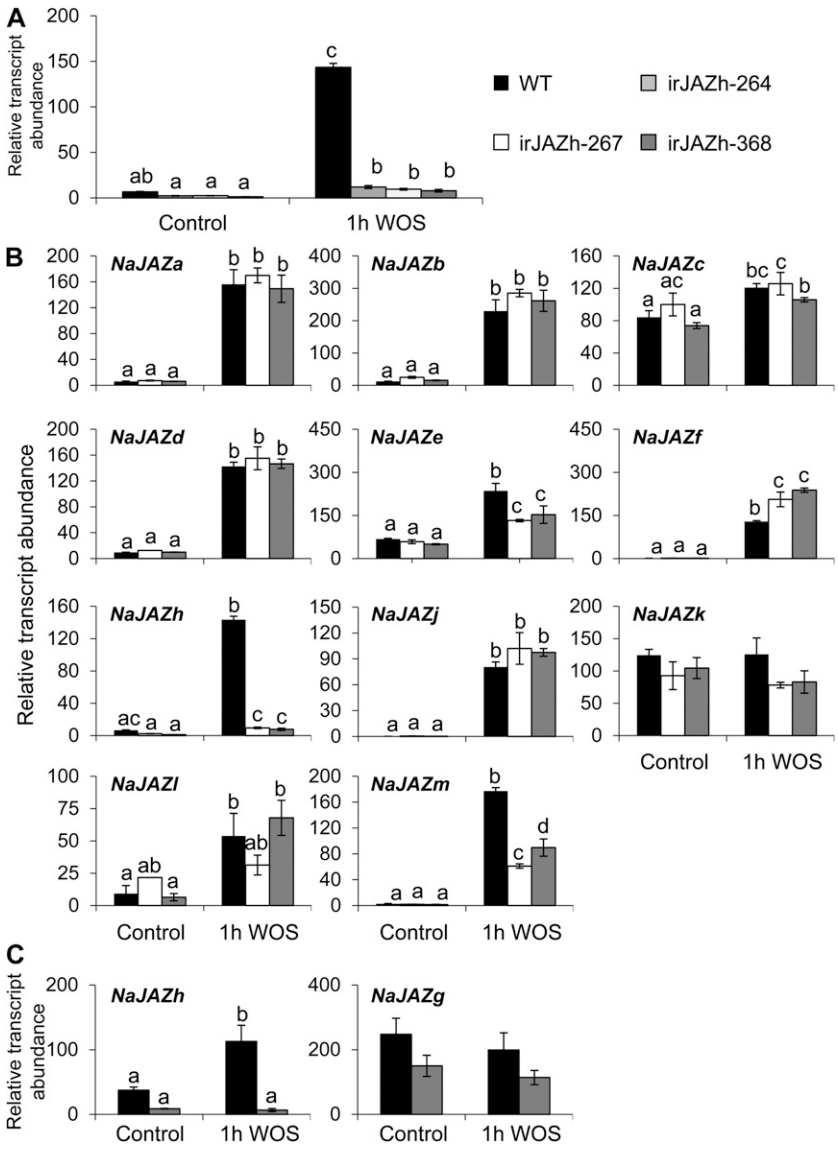

Figure 3. Silencing of the *NaJAZh* gene affects the expression of several other *NaJAZ* genes in *N. attenuata*. A, Transcript abundances of the *NaJAZh* gene were determined by real-time qPCR in three independent silenced irJAZh lines before and after elicitation with W+OS. B, Transcript abundances of other *NaJAZ* genes determined by qPCR in untreated (Control) and 1-h W+OS-elicited (1h WOS) leaves of irJAZh plants. C, *NaJAZh* and *NaJAZg* expression in systemic roots of irJAZh plants. Bars indicate *EF1a*-normalized relative transcript abundances ± SE ($n = 3$). Different letters (a–d) indicate significant differences among the combination of genotypes (wild type [WT] versus independent irJAZh lines irJAZh-264, -267, and -368) and treatments determined by ANOVA ($P \leq 0.05$).

herbivore performance bioassays using the specialist herbivore *M. sexta* and irJAZh plants. Because JAZ proteins likely repress defense genes, their absence should result in strong constitutive defense responses in JAZ-silenced plants. To examine the behavior of young as well as older irJAZh plants (showing necrotic symptoms, as described later), we placed one *M. sexta* neonate per leaf on 20 and 10 replicates of rosette and flowering stage, respectively, irJAZ and wild-type plants. The mass of caterpillars was first determined at 5 d and then every 2 d until 13 d (Fig. 4). NaJAZh silencing strongly suppressed the performance of *M. sexta* specialist herbivores, both in young and older plants; however, the growth of larvae was retarded to a greater degree on mature irJAZh plants. These results suggested that irJAZh plants are better defended against specialist herbivores, presumably due to the high levels of defense metabolites in these plants.

Before analyzing the levels of direct defense metabolites, we determined if changes in upstream JA and JA-Ile accumulations and/or metabolism could be responsible for the extraordinary defense properties of irJAZh plants. The levels of JA, JA-Ile, abscisic acid (ABA), and salicylic acid (SA) were measured in W+OS-elicited leaves of rosette stage irJAZh-264, -267, and -368 plants and wild-type plants at 0, 1, 2, and 3 h after oral secretion elicitation (Fig. 5). Whereas the content of JA was significantly higher in irJAZh plants compared with wild-type plants at 1 h post elicitation, JA-Ile levels in irJAZh leaves did not differ from those in wild-type plants. Similar to JA-Ile, the levels of SA and ABA did not differ significantly between irJAZh and wild-type plants. Because JA-Ile is the active form of JA in the signaling process, we assumed that higher JA levels would not be directly responsible for the strongly elevated resistance of irJAZh plants.

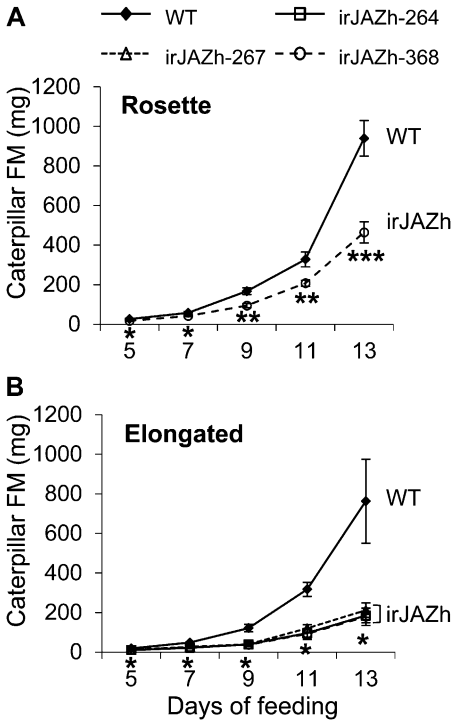

Figure 4. The performance of larvae of the specialist herbivore *M. sexta* is strongly suppressed on irJAZh plants. The performance of *M. sexta* larvae was observed on the wild type (WT) and NaJAZh-silenced lines at two stages of development. A, *M. sexta* neonates were placed on rosette-stage leaves of wild-type and irJAZh-368 plants. The mean fresh mass (FM) ± SE of irJAZh-368 caterpillars ($n = 20$) was significantly smaller at all time points as determined by Student's t test (* $P \leq 0.05$, ** $P \leq 0.01$, *** $P \leq 0.001$). B, *M. sexta* performance ($n = 10$) on early-flowering-stage wild-type plants and three independent JAZh-silenced lines (irJAZh-264, -267, and -368) that developed necrotic lesions during the experiment. Significant differences between genotypes were determined at each time point by ANOVA (* $P \leq 0.05$).

Silencing of NaJAZh Shows a Differential Effect on Direct Defenses in *N. attenuata*

To evaluate if the substantially elevated herbivore resistance of irJAZh plants was due to higher levels of toxic defense metabolites in these plants, we examined trypsin protease inhibitor (TPI) activity (Jongsma et al., 1994, 1995; Habib and Fazili, 2007) and the accumulation of the secondary metabolites nicotine (Shoji et al., 2000; Steppuhn et al., 2004) and 17-hydroxygeranyllinalool diterpene glycosides (DTGs; Jassbi et al., 2008; Heiling et al., 2010) in W+OS-elicited irJAZh and wild-type plants (Fig. 6). The basal levels of TPI activity in irJAZh plants were already six to 10 times higher compared with wild-type plants, and these levels remained approximately five times higher in 72-h W+OS-elicited irJAZh leaves (Fig. 6A). The pooled DTG levels in irJAZh plants, determined by HPLC, showed accumulation patterns similar to TPI activity (Fig. 6B). In particular, the constitutive levels of DTGs in uninduced irJAZh plants were dramatically higher compared with wild-type plants. Both constitutive and induced levels of nicotine in leaf tissues were surprisingly reduced in irJAZh compared with wild-type plants already at constitutive uninduced levels (Fig. 6C). When we checked the root expression of *N. attenuata* putrescine-*N*-methyltransferase (*NaPMT*) involved in nicotine biosynthesis, and nicotine levels in the roots, they were not significantly different between roots of uninduced wild-type and irJAZh plants (Supplemental Fig. S5). We also examined the levels of other potentially important defense-related secondary metabolites, including dicaffeoylspermidine (DCS) and caffeoylputrescine (CP) in irJAZh plants (Kaur et al., 2010). Whereas CP levels appeared higher at 72 h in W+OS-elicited irJAZh plants, DCS levels were not significantly different between wild-type and irJAZh plants (Supplemental Fig. S6).

A shift from core to dimalonylated DTGs after herbivore attack is a typical JA-regulated (and COI1-dependent) process in *N. attenuata* plants (Heiling et al., 2010). To see how DTGs are regulated in irJAZh plants, we measured DTG levels by a more sensitive, high resolution liquid chromatography-electrospray ionization-tandem mass spectrometry (LC-ESI-MS/MS) method (Fig. 7) that allowed relative quantification of individual DTGs subdivided into precursor, core, single-malonylated, and dimalonylated groups (listed in the putative order of biosynthesis; Heiling et al., 2010). Interestingly, the irJAZh plants showed very high basal levels of precursor and core DTGs (Fig. 7;

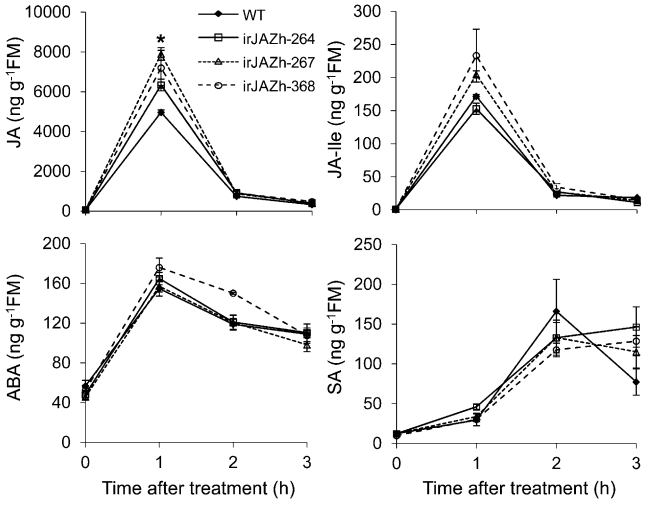

Figure 5. NaJAZh silencing does not alter JA-Ile levels induced by simulated herbivory. Rosette-stage plants (the wild type [WT] and NaJAZh-silenced lines irJAZh-264, -267, and -368) were treated with simulated herbivory (W+OS) and harvested before and 1, 2, and 3 h after elicitation. Mean ± SE levels of JA, JA-Ile, ABA, and SA ($n = 3$) were determined by LC-ESI-MS/MS using internal deuterium-labeled hormone standards. JA levels were significantly higher at 1 h after elicitation in irJAZh lines, but other hormones showed no significant differences compared with wild-type plants. Asterisks indicate significant differences among the wild type and independent irJAZh lines determined by ANOVA (* $P \leq 0.05$). FM, Fresh mass.

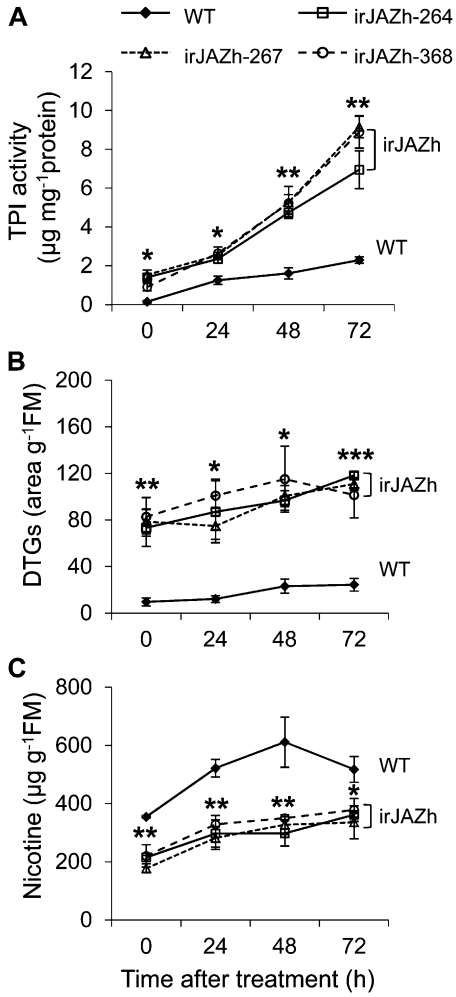

Figure 6. NaJAZh silencing enhanced constitutive and inducible levels of TPIs and DTGs but suppressed nicotine accumulation. Rosette-stage plants (the wild type [WT] and NaJAZh-silenced lines irJAZh-264, -267, and -368) were treated with simulated herbivory (W+OS), and treated leaves were harvested before and 24, 48, and 72 h after elicitation. Mean ± SE levels of TPIs determined by radial diffusion assay (A) and DTGs determined by HPLC (B) were significantly higher at each time point in irJAZh compared with wild-type plants. Mean ± SE levels of nicotine (C) determined by HPLC were significantly lower in irJAZh compared with wild-type plants at every time point (ANOVA; * $P \leq 0.05$, ** $P \leq 0.01$, *** $P \leq 0.001$; $n = 3$). There were no significant differences found in metabolite content when three independent irJAZh lines were compared. FM, Fresh mass.

0-h time point), which quickly declined after W+OS elicitation of the plants. Subsequently, W+OS treatment increased the single-malonylated and dimalonylated DTG levels, both in irJAZh and wild-type plants; however, the levels in irJAZh were dramatically higher. These results suggest that although irJAZh plants can constitutively accumulate a large amount of DTG precursors, another JA-dependent signal(s) may be required for their conversion to malonylated and dimalonylated forms during herbivore attack.

To further examine the role of NaJAZh in the regulation of secondary metabolism under real herbivory attack, we analyzed the leaves from wild-type and irJAZh plants that were exposed to *M. sexta* feeding for 5 d. The accumulation of total DTGs and nicotine was consistent with the previous W+OS elicitation results, showing significantly higher levels of DTGs and lower nicotine levels in herbivore-attacked leaves of irJAZh compared with wild-type plants (Supplemental Fig. S7).

irJAZh Plants Release More Volatile Compounds

The releases of GLVs and VOCs are typical herbivory-induced responses in *N. attenuata* plants (Halitschke et al., 2000; Kessler and Baldwin, 2001; Baldwin et al., 2002; Paschold et al., 2006). To determine if *NaJAZh* also regulates volatile emissions, we collected GLVs and VOCs released from the leaves of irJAZh and wild-type plants over 24 h, both before and after W+OS elicitation (Fig. 8). The irJAZh plants released more GLVs (e.g. cis-3-hexenylacetate and cis-3-hexenylbutyrate); however, the most remarkable differences were found in terpenoid emissions (VOCs) of these plants. For example, the sesquiterpenes trans-α-bergamotene and trans-β-farnesene were strongly elevated, especially in the case of W+OS-elicited irJAZh plants. These data suggest that NaJAZh, apart from regulating the accumulation of direct defense metabolites like TPIs and DTGs, also regulates the volatile emissions that are known to function as an indirect defense against herbivores in *N. attenuata* plants.

Global Transcriptional Changes Associated with NaJAZh Silencing in *N. attenuata*

As we have shown above, NaJAZh silencing strongly altered defensive metabolite profiles in *N. attenuata* leaves. To gain more insight into the mechanisms (and genes) involved in defense against herbivores, we compared global gene expression by microarrays using irJAZh-368 and wild-type leaf samples 2 h after W+OS elicitation. NaJAZh silencing altered the expression of a large number of genes (188 out of 43,503 microarray probes were at least 3-fold up-regulated [97 genes] or down-regulated [91 genes] in irJAZh plants compared with wild-type plants). As predicted from the strong defense profile of irJAZh plants, a number of the 58 functionally annotated up-regulated genes could be assigned to volatile emission or defense-related functional categories (Supplemental Table S1). For example, the six-domain trypsin inhibitor precursor (3.9-fold), 5-epi-aristolochene synthase (5.2-fold), and γ-thionin-defensin-like protein (30.1-fold) were strongly up-regulated after W+OS treatment in irJAZh compared with wild-type plants. Furthermore, the primary metabolism and signal transduction genes (nitrate transporter, 5.2-fold; *A. thaliana* chlorophyllase2, 3.3-fold; basic helix-loop-helix family protein, 4.6-fold) were among the strongly regulated targets of the NaJAZh repressor. Similar to previous qPCR analysis (Fig. 3), NaJAZh silencing modulated the expression of several

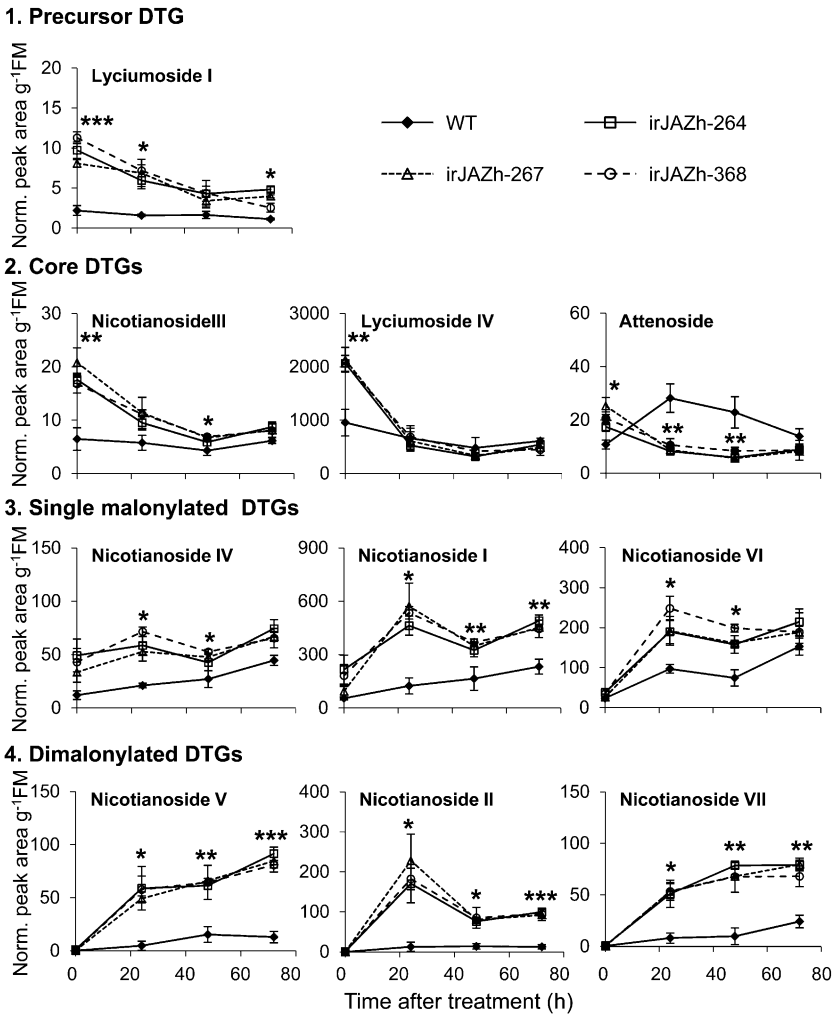

Figure 7. NaJAZh silencing strongly affects the accumulation and structural modification of DTGs in transgenic plants. Rosette-stage plants in the glasshouse were treated with simulated herbivory (W+OS) and harvested before and 24, 48, and 72 h after elicitation. Mean ± SE relative amounts of individual DTGs were determined by LC-ESI-MS/MS. The malonylated DTGs (rows 3 and 4) strongly accumulated after treatment in all three independent irJAZh lines (irJAZh-264, -267, and -368) compared with wild-type (WT) plants, whereas core (row 2) and precursor (row 1) DTGs were highest in the irJAZh lines before treatment (constitutive levels at 0 h). Asterisks indicate significant differences among the wild type and three independent irJAZh lines determined by ANOVA (* $P \leq 0.05$, ** $P \leq 0.01$, *** $P \leq 0.001$; $n = 3$). There were no significant differences found in metabolite content among three independent irJAZh lines. FM, Fresh mass.

other *JAZ* genes (*NaJAZf*, up 4.6-fold; *NaJAZj*, up 3.6-fold; Supplemental Fig. S4).

NaJAZh silencing also resulted in the repression of 52 functionally annotated genes in irJAZh plants compared with wild-type plants (greater than 3-fold change; Supplemental Table S2). As expected, *NaJAZh* was among the strongly suppressed genes (3.4-fold). Interestingly, NaJAZh silencing resulted in the down-regulation of genes from similar categories, as already found in the up-regulated gene list (e.g. monoterpene synthase 2, 8.3-fold), consistent with a complex metabolic reconfiguration and possible redirection of metabolic fluxes within the same metabolic pathways during defense (e.g. monoterpene versus sesquiterpene biosynthesis).

NaJAZh Silencing-Induced Leaf Necrosis at Late Developmental Stages

NaJAZh silencing did not affect the growth and development of *N. attenuata* plants until the elongation stage, when the strongly silenced irJAZh lines displayed spontaneous necrotic lesions on the leaves. This necrotic phenotype was observed in five independent irJAZh transgenic lines, therefore excluding the possibility that it was the consequence of the random insertion of a NaJAZh-silencing construct into another independent gene in the *N. attenuata* genome.

The symptoms first appeared as small necrotic spots on cotyledons that gradually spread to older leaves, after the development of the leaves (Fig. 9). Late in development, all leaves but not flowers or seed capsules of irJAZh plants were typically engulfed by the necrosis in strongly silenced irJAZh lines (Fig. 9). To a large extent, the degree of necrosis was dependent on the transgenic line used in the experiment (with the strongest symptoms observed in irJAZh-368), and the necrotic symptoms were completely lost when the irJAZh-267 plants (showing strong necrosis in irJAZh homozygous plants) were crossed with the wild type to create a hemizygous cross (Supplemental Fig. S8). We interpret these results to mean that a low threshold level of *NaJAZh* expression can possibly counteract the development of necrotic symptoms. Although not addressed in this work, the hypothesis that accumulations

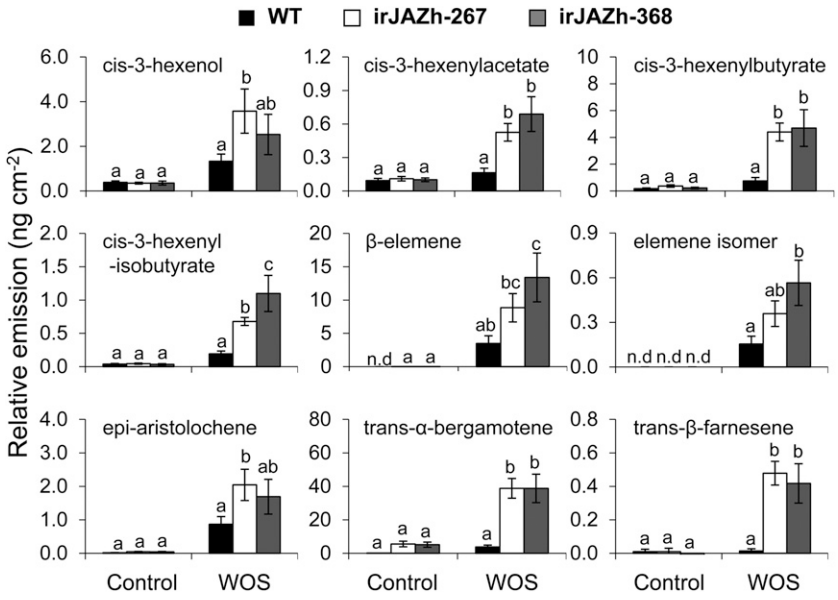

Figure 8. NaJAZh-silenced plants emit higher amounts of VOCs and GLVs. Volatiles were collected from the head space of wild-type (WT) and irJAZh (irJAZh-267 and -368) leaves for 24 h after connecting the volatile trap units to locally treated leaves 3 h after W+OS elicitation; control plants were collected in parallel but remained untreated. Samples were analyzed by gas chromatography-mass spectrometry with tetraline as an internal standard. Bars indicate normalized relative emissions of volatiles per cm^2 of leaf area ± SE ($n = 5$). Different letters (a–c) indicate statistically significant differences in emissions among genotypes (the wild type versus two independent irJAZh lines) and treatments determined by ANOVA ($P \leq 0.05$). n.d, Not detected.

of some toxic intermediate in nicotine biosynthesis, shown to be impaired in irJAZh plants, could be responsible for the lesions in older leaves should be thoroughly examined.

Reactive Oxygen Species Accumulation in Wounded Leaves

Reactive oxygen species (ROS) are common markers of programmed cell death (PCD) and necrosis in plants (Allan and Fluhr, 1997; Desikan et al., 1998; Beers and McDowell, 2001; Houot et al., 2001; Mittler et al., 2004; Cheeseman, 2007). To determine if the necrotic lesions in irJAZh plants could be due to the activation of ectopic PCD in irJAZh plants, we first analyzed the hydrogen peroxide (H_2O_2) levels in leaves of two independent NaJAZh-silenced lines (irJAZh-267 and -368) and compared them with wild-type H_2O_2 levels. We used presymptomatic unwounded leaves as well as puncture-wounded leaves detached from mature plants and stained them with the H_2O_2-sensitive indicator diaminobenzidine (DAB); the leaves were floated on staining solution overnight in darkness and destained the next day in a clearing solution to visualize the brown precipitate of oxidized DAB (Fig. 10A). A stronger DAB staining in the unwounded leaves of irJAZh compared with wild-type plants was readily observed. Although the wound-induced accumulation of H_2O_2 appeared as dark brown circles around puncture wounds on the leaves, these circles were significantly more intense in irJAZh compared with wild-type leaves, suggesting that irJAZh plants are subjected to strong oxidative stress due to the high ectopic accumulation of H_2O_2 in their leaves.

Because DAB staining requires a long incubation of the leaves in the staining solution, which may have caused some artifacts in observed H_2O_2 accumulation patterns, we also quantified the H_2O_2 accumulation in wounded leaves using the more sensitive Amplex Red kit, which allows more precise determination of the immediate levels of H_2O_2 (Fig. 10B). In addition to significantly higher basal levels of H_2O_2 found in the irJAZh leaves (Fig. 10B; 0 h), we detected a strong burst of H_2O_2 after wounding that occurred only in irJAZh plants. We conclude that the NaJAZh protein is essential for the suppression of both basal and wound-induced ROS in mature *N. attenuata* leaves.

Gene Expression during Necrosis in irJAZh Leaves

To further examine the possible mechanisms involved in leaf necrosis in irJAZh plants, we measured the expression of *NaJAZh* and three known PCD markers in tobacco (harpin-induced1 [Hin1], hypersensitivity-related203 [Hsr203], and *N. attenuata* vacuolar processing enzyme361 [NaVPE361]) using a time-resolved kinetic of leaf samples from irJAZh and wild-type plants (Fig. 10C). In this experiment, we first labeled one rosette leaf growing at the −1 node (one position younger than the leaf undergoing the source-sink transition) of 34-d-old irJAZh and wild-type plants, well before the development of necrotic symptoms on irJAZh plants was observed. Subsequently, we kept collecting sets of labeled leaves in 2-d intervals until necrotic lesions appeared on labeled leaves of irJAZh plants. As expected, irJAZh plants showed low expression of *NaJAZh* throughout the experiment, consistent with the stable silencing genotype of these plants. Interestingly, whereas wild-type plants showed a relatively constant expression of the *NaJAZh* gene, the transcript levels suddenly increased at 50 d post germination, when the full necrosis phenotype was observed in

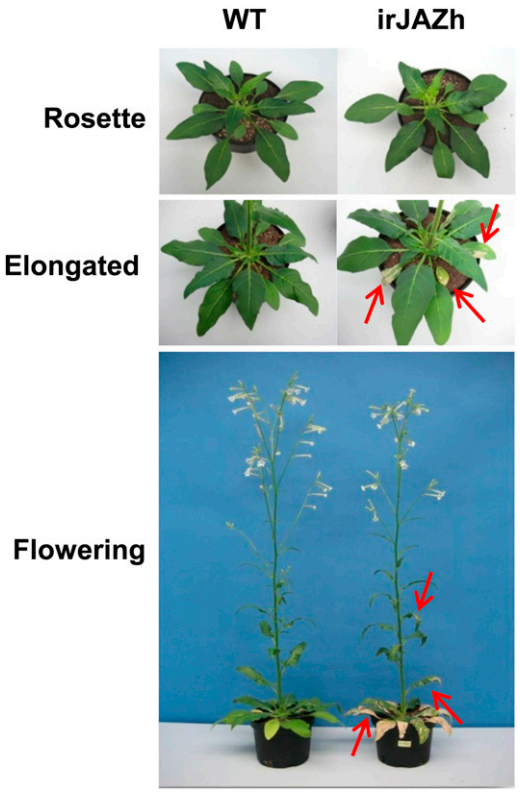

Figure 9. Elongated and mature irJAZh plants develop spontaneous necrosis on leaves. Necrotic spots on leaves of irJAZh plants (indicated by red arrows) appeared in a strict developmental sequence as irJAZh plants started to elongate and transitioned into the flowering stage of growth. Symptoms were first detected on cotyledons of irJAZh plants and gradually spread to the next developed but still fully green leaves. Necrotic lesions were not detected on flowers or capsules of the irJAZh plants. In contrast to irJAZh plants, wild-type (WT) plants developed natural senescence that was characterized by yellow color of the old leaves and necrosis of the yellow senescent leaves in the final stages of development.

irJAZh leaves (Fig. 10, C and D; the arrows depict the first day when the labeled irJAZh leaves showed visible necrotic spots on their lamina). At the same time, the expression of the PCD marker genes *Hin1*, *Hsr203*, and *NaVPE361* spiked in irJAZh plants but not in wild-type plants. Because *VPE* genes are involved in the vacuole collapse that triggers hypersensitive cell death in plants (Hatsugai et al., 2004; Hara-Nishimura et al., 2005), NaJAZh, directly or indirectly, contributed to the suppression of cell death in mature *N. attenuata* leaves.

Next, we examined if the necrotic symptoms could be associated with the unbalanced phytohormone levels in irJAZh leaves, using the same set of samples used in gene expression analysis. Although JA and ABA levels were fairly normal in irJAZh plants, we found a strong increase in SA levels that coincided with the development of necrosis on irJAZh leaves (Fig. 10D). However, it was not clear if the accumulation of SA was the cause or consequence of PCD in irJAZh leaves. As necrotic symptoms on irJAZh plants always spread in a strictly ontogenetic order, affecting the oldest leaves found on the plant, the possibility of a senescence-related origin of PCD in irJAZh plants seemed very likely, a hypothesis examined next.

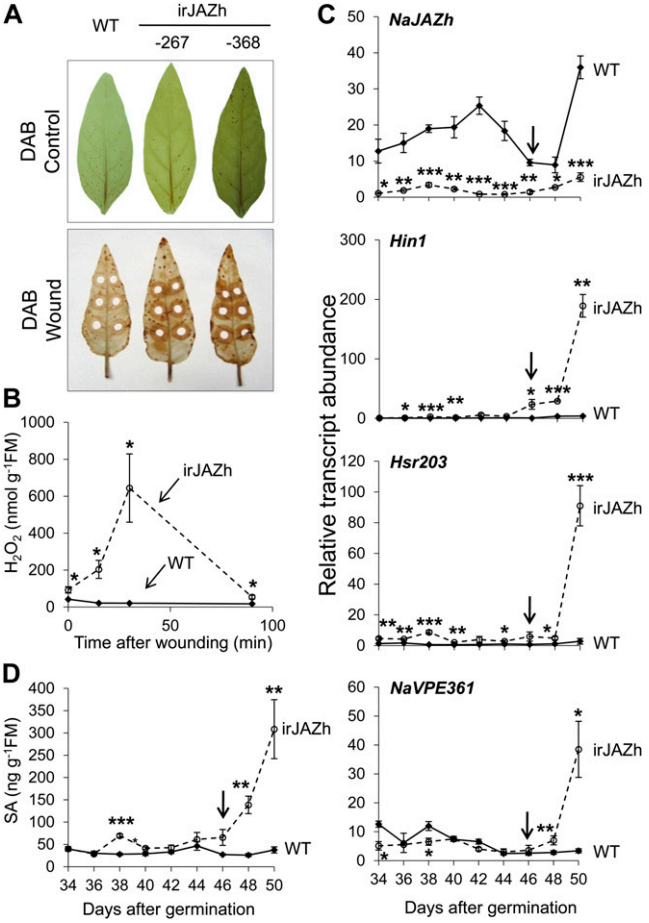

Figure 10. irJAZh plants accumulate ROS and express PCD markers during leaf necrosis. A, For DAB staining, leaves were detached from plants and either punched with a cork borer to wound (bottom panel) or leaves remained unwounded (top panel). The entire leaf was floated in DAB staining solution overnight in the dark and destained to visualize the brown DAB precipitate. B, For the Amplex Red assay, leaf extracts prepared from wounded leaves of irJAZh-368 and wild-type (WT) plants were incubated with Amplex Red reagent. Amplex signal intensity was determined by measuring sample fluorescence at excitation/emission = 530/590 nm. Mean ± SE levels of H_2O_2 ($n = 3$) were calculated using H_2O_2 external calibration curves, and significant differences between wild-type and irJAZh plants were determined by Student's *t* test at every measured time point (* $P \leq 0.05$). C, Mean relative transcript abundances ± SE of *NaJAZh* and PCD marker genes (*Hin1*, *Hsr203*, and *VPE361*) in developing *N. attenuata* plants (34–50 d post germination; $n = 4$). D, SA levels determined by LC-ESI-MS/MS in developing *N. attenuata* plants (34–50 d post germination; $n = 4$). Arrows in C and D indicate the date of the first appearance of necrotic symptoms of a leaf that during early rosette-stage growth (34 d post germination) occupied a node one position younger than the source-sink transition leaf (−1). Asterisks in C and D indicate significant differences between wild-type and irJAZh plants determined by Student's *t* test (* $P \leq 0.05$, ** $P \leq 0.01$, *** $P \leq 0.001$). FM, Fresh mass.

Necrotic Lesion Symptoms in irJAZh Plants Are Suppressed by High Nitrogen Availability in Soil

If the necrosis was a result of exaggerated natural senescence in irJAZh plants, we assumed that a delay in senescence should slow or even prevent the development of necrosis on irJAZh leaves. Therefore, we planted irJAZh and wild-type plants in soil as before and supplied (in watering solution) one group of the plants with 50 mL of 20 mM ammonium nitrate solution every 2 d to delay the senescence process in these plants. As expected, the treatment resulted in dark green leaves in the nitrate-supplied group of both irJAZh and wild-type genotypes (Fig. 11A), and greening of irJAZh plants strongly suppressed the appearance of necrotic symptoms observed on 45-d-old irJAZh plants, when the control group of irJAZh plants displayed a clear necrotic phenotype. In later stages of development, although necrosis also developed on nitrate-supplied irJAZh plants, it was significantly milder compared with plants grown under a normal glasshouse fertilization regime. Interestingly, watering with nitrate solution applied to mature elongated plants in soil could stop the spread of already initiated necrosis on the irJAZh leaves, leading to recovery and normal growth of the leaves. Rejuvenation of irJAZh plants was capable of counteracting the leaf necrosis, suggesting that an out-of-control senescence process could be responsible for the necrotic phenotype of irJAZh plants. When we measured the chlorophyll content in selected rosette leaves starting from 35 d post germination until the development of necrosis on irJAZh leaves (approximately 50 d post germination; Fig. 11B), the chlorophyll content started to decline in both wild-type and irJAZh plants just before the first necrotic symptoms in irJAZh plants. We assume that plants may initiate the natural senescence process at this point, which is tempered by the function of the *NaJAZh* gene in wild-type plants.

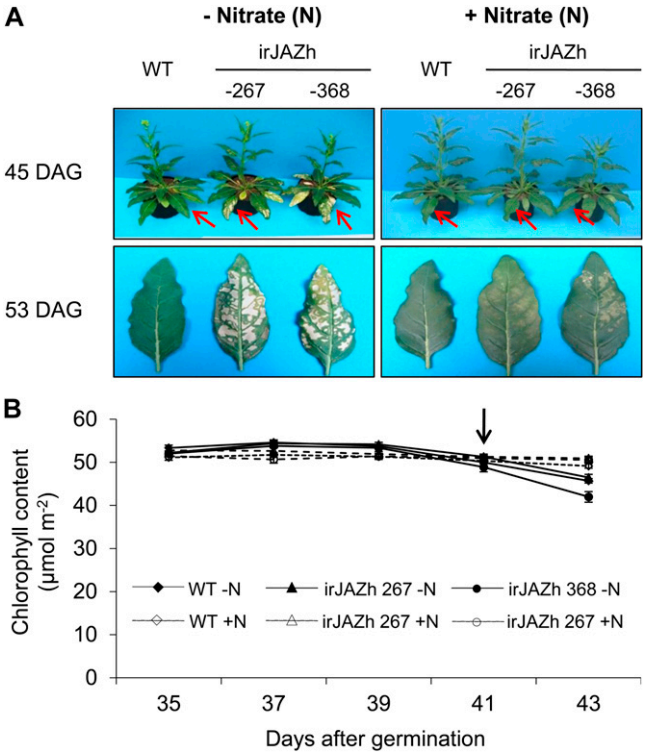

Figure 11. Rejuvenation of irJAZh plants delays the development of necrosis on the leaves. A, The extent of necrotic lesions was documented in wild-type (WT) and irJAZh (irJAZh-267 and -368) plants at 45 and 53 d post germination. Plants were cultivated either under the normal glasshouse fertilization regime (Peters Allrounder and Borax; left panel) or under high nitrogen supply rates (supplied with an additional 50 mL of 20 mM NH_4NO_3 every 2 d starting at 30 d post germination [DAG]; right panel). Arrows indicate the leaf that during early rosette-stage growth (34 d post germination) occupied a node one position younger than the source-sink transition leaf (−1) and was used to measure chlorophyll contents. B, Mean ± SE chlorophyll content ($n = 5$) in wild-type and irJAZh (irJAZh-267 and -368) leaves determined between 35 and 43 d post germination. The arrow indicates the date of the first visible necrotic symptoms on the labeled leaf. Chlorophyll content started to decline when the first necrotic symptoms appeared on irJAZh plants grown under the normal glasshouse fertilization regime; compared with 39 d, the chlorophyll content at 41 d post germination significantly decreased in all plants grown under the normal fertilization regime (determined by Student's t test; $P \leq 0.01$). [See online article for color version of this figure.]

Performance and Metabolism of NaJAZh-Silenced Plants in Nature

Lastly, we wanted to know if the unbalanced defense of irJAZh plants could influence the performance of these plants when grown in the native habitat of *N. attenuata* in the Great Basin Desert of Utah. Although the silencing efficiency and the main metabolic features of irJAZh plants were preserved in the field (Supplemental Figs. S9–S12), damage inflicted by native herbivores on irJAZh plants was not significantly different from the empty vector (EV) plants that were planted in a paired size-matched design with the irJAZh plants in the field (Supplemental Fig. S13). Similar to "naive" glasshouse plants (Fig. 7), field-grown irJAZh plants also accumulated much more of the core, single-malonylated, and dimalonylated DTGs, but not the DTG precursor lyciumoside I. This suggests that exposure to natural herbivory in the field may have shifted the DTG pools in irJAZh plants toward modified forms on account of precursor lyciumoside I (Supplemental Fig. S11). We also observed some differences in volatile profiles of irJAZh plants under field and glasshouse conditions. Whereas the trans-α-bergamotene content was still substantially elevated as in glasshouse irJAZh plants (Fig. 8), the field plants did not release elevated amounts of trans-β-farnesene (Supplemental Fig. S12). H_2O_2 accumulation in the leaves was still higher in irJAZh compared with EV plants (Supplemental Fig. S14), but necrotic lesions never developed under field conditions (Supplemental Fig. S15). We assume that the levels of JAZh silencing

determined in the field (Supplemental Fig. S9) were below the threshold levels required for tissue damage and lesion formation. Alternatively, field plants that were grown under approximately twice the photosynthetically active radiation levels of glasshouse-grown plants may have activated stronger antioxidant protection that restricted necrosis in irJAZh plants.

DISCUSSION

Since the recent discovery of JAZ proteins as repressors of JA signaling, functional characterization of *JAZ* genes has mainly been performed in Arabidopsis. However, the phenotypes associated with the silencing of individual *JAZ* genes in Arabidopsis have rarely been reported (for review, see Pauwels and Goossens, 2011). When we silenced a newly identified *JAZh* gene in *N. attenuata*, a strong derepression of direct (TPIs and DTGs) and indirect (volatile emissions such as terpenoids) defense responses was observed, whereas the accumulation of another defense metabolite, nicotine, was reduced. In addition, irJAZh plants displayed an unexpected necrotic lesion phenotype during late growth and maturation. Although the silencing of NaJAZh strongly deregulated defense responses in *N. attenuata*, it still remains to be determined which of the phenotypes observed in irJAZh plants are directly controlled by the NaJAZh repressor and which result from the regulatory function of JAZh over the other JAZ proteins in *N. attenuata*.

Identification and Expression of *JAZ* Genes in *N. attenuata*

Seven novel JA-inducible genes containing the ZIM domain, previously implicated in the regulation of transcription in Arabidopsis (Shikata et al., 2004), were identified by microarrays of methyl jasmonate (MeJA)-treated plants and, as a consequence, were classified as a novel JAZ protein family (Thines et al., 2007). Using a sequence homology search, five additional JAZ proteins were identified in the Arabidopsis genome, based on the presence of characteristic structural motifs, ZIM and Jas (Thines et al., 2007, Yan et al., 2007). In this report, using a similar strategy, we found 12 putative *JAZ* genes in *N. attenuata* that complement three previously identified proteins, JAZ1, JAZ2, and JAZ3, from *N. tabacum* (Shoji et al., 2008). All *NaJAZ* genes were expressed in aboveground and/or belowground tissues after W+W or W+OS treatment (Fig. 2) or even without treatment. Our results, summarized in Figure 2, are consistent with previous studies showing that the expression of most *JAZ* genes is inducible by local wounding and/or herbivore feeding (Chung et al., 2008; Shoji et al., 2008; Koo et al., 2009), which propagates to systemic uninduced leaves, similar to *AtJAZ5* and *AtJAZ7* genes (Koo et al., 2009).

Alternative splicing of *JAZ* genes was proposed to play an important role in JAZ/COI1 interactions and JA signaling in Arabidopsis (Chung and Howe, 2009; Chung et al., 2010). Two differentially spliced forms of the AtJAZ10 protein show differential binding affinity to SCF^{COI1}, suggesting that alternative splicing of *JAZ* genes may be contributing to the fine-tuning of JA-dependent responses. During the cloning of *N. attenuata JAZ* genes, we also retrieved cDNA clones with variable lengths in at least two cases, *NaJAZc* and *NaJAZk*. While NaJAZc proteins differed in the presence of an internal 32-amino acid sequence (NaJAZc.1 and NaJAZc.2), NaJAZk occurred in two forms, one that completely lacked the Jas motif (NaJAZk.2) and another that contained an incomplete Jas sequence (NaJAZk.1; Supplemental Fig. S1). Further analysis of alternatively spliced forms of tobacco JAZ proteins and completion of the tobacco genome will be required to understand the function of these modifications in the regulation of JA signaling.

NaJAZh Controls a Subset of Direct and Indirect Defense Responses

Because JAZ proteins repress JA-dependent responses, plants lacking JAZ function should be displaying stronger and constitutive accumulation of anthocyanins or should have altered pollen development, senescence, and root responses (Mandaokar et al., 2006; Balbi and Devoto, 2008; Howe and Jander, 2008; Browse, 2009; Reinbothe et al., 2009; Shan et al., 2009; Qi et al., 2011; Song et al., 2011). When Thines et al. (2007) examined the effect of several single JAZ knockouts or ectopically overexpressed *JAZ* genes in Arabidopsis, no strong phenotypic changes were observed in these lines, revealing a functional redundancy of JAZ proteins in plants. In contrast, Jas domain-truncated (dominant negative) forms of JAZ proteins produced several of the expected phenotypes, including male sterility and insensitivity to JA in root inhibition assays (Chini et al., 2007; Thines et al., 2007; Chung and Howe, 2009). A higher sensitivity to JA resulting in stronger suppression of root growth was also observed in transgenic lines with reduced *AtJAZ1* (Grunewald et al., 2009) and *AtJAZ10* (Yan et al., 2007; Demianski et al., 2012) expression. In addition, a knockdown line of AtJAZ10 became more susceptible to *Pseudomonas syringae* DC3000 infection (Demianski et al., 2012).

Previously, a dominant negative form of NtJAZ1 and NtJAZ3 proteins, equivalents of NaJAZd and NaJAZa, respectively, repressed the MeJA-induced accumulation of nicotine and related alkaloids in tobacco hairy roots and cell cultures (Shoji et al., 2008); however, no other defense metabolites were reported in these experiments. In this report, irJAZh transgenics silenced in the expression of a single *JAZ* gene in *N. attenuata* accumulated and released abnormally high levels of constitutive direct (and indirect) defense metabolites, which was further amplified by oral secretion elicitation. While irJAZh plants were deficient in

nicotine accumulation, cross talk among individual JAZ-regulated defense responses in tobacco was revealed. The reduced nicotine contents in irJAZh plants and the generally negative role of JAZ in nicotine accumulation (Shoji et al., 2008) suggests a branched regulation of JA-mediated defense metabolites in tobacco controlled by separate JAZ proteins.

Cross Talk in the JAZ Regulatory Network

NaJAZh silencing resulted in profound changes in direct and indirect defense profiles of *N. attenuata* plants. We first suspected that such a broad phenotype could be the result of nonspecific cross-silencing of other *JAZ* genes by the irJAZh construct. Nevertheless, we rechecked the expression of *NaJAZ* genes in wild-type and NaJAZh-silenced plants (Fig. 3B; determined by qPCR). Two genes, *NaJAZe* and *NaJAZm*, showed reduced gene expression, together with *NaJAZh* at 1 h after W+OS elicitation. However, no other *JAZ* gene except for *NaJAZh* was found to be significantly reduced in irJAZh plants at 2 h after W+OS treatment, which was determined by an independent microarray approach (Supplemental Fig. S4). In addition, we observed the induction of *NaJAZf* expression at 1 h after W+OS in irJAZh plants, which persisted even at 2 h after W+OS elicitation. Therefore, it is very likely that NaJAZh silencing directly or indirectly affected the expression of other *JAZ* genes, which was not the result of a cross-silencing effect. In Arabidopsis, promoter regions of many *JAZ* genes contain G-box sequences, a known target sequence of MYC2 proteins (Chini et al., 2007), which provides a possible mechanism for cross talk and the mutual regulation of *JAZ* genes in JA signaling. Subsequently, some of the observed phenotypes associated with NaJAZh silencing could be attributed to the function of other *JAZ* genes that were deregulated by silencing of NaJAZh.

The results of our transcriptional studies were further supported by the reduction of nicotine levels in irJAZh plants. Because nicotine is synthesized in the roots and subsequently transported to leaves through the xylem stream (Baldwin et al., 1997; Wink and Roberts, 1998), we assume that nicotine biosynthesis is regulated independently from defense metabolites that are directly expressed in the leaves (TPI, DTGs, and volatiles). Recently, increased root expression of *AtJAZ1*, *AtJAZ2*, and *AtJAZ9* genes was reported in Arabidopsis after local wounding (Hasegawa et al., 2011; Sogabe et al., 2011). Possibly, a subset of JAZ proteins may have a specific function in the root tissues. Because the *NaJAZf* gene was up-regulated after W+OS induction in irJAZh plants, we speculate that this gene could be involved in the control of the biosynthesis and/or transport of nicotine in tobacco plants. The most likely targets of this JAZ would be the root-expressed *MYC2*-like genes in tobacco and/or AP2/ERF TFs reported as positive regulators of nicotine biosynthesis in tobacco (Shoji et al., 2010; Shoji and Hashimoto 2011; Zhang et al., 2012).

The irJAZh Phenotype Is Robust But Not Beneficial for Field-Grown Plants

A number of previous studies demonstrated that plants use inducible defense as a resource-saving strategy (Cipollini and Bergelson, 2001; Strauss et al., 2002; Cipollini et al., 2003; Zavala et al., 2004b). However, the time delays required to accumulate defensive quantities of metabolites could be a significant drawback of the inducible deployment of defenses. Because irJAZh plants expressed high constitutive and stronger inducible defenses compared with wild-type plants, we were curious whether these "super-defenders" would perform better in the native habitat of *N. attenuata* in the Great Basin Desert, an environment characterized by its extremely variable and stressful conditions. However, in two field seasons, we did not observe any evidence for higher anti-herbivore defense in irJAZh plants that were planted together with EV control plants in the field plot (Supplemental Fig. S13). This suggests that, under natural conditions, constitutively higher TPI and DTG levels did not provide any real advantage to irJAZh plants compared with EV plants (mainly dependent on their inducible defenses). In other words, the Utah ecotype of *N. attenuata* used in this study may have already been equipped with the most efficient defense system, and the time lags associated with defense deployment do not significantly compromise the plant's ability to defend against herbivores in nature. In addition, several alternative hypotheses need to be examined, such as whether the lower nicotine levels in irJAZh plants or the priming of EV plants by natural herbivores in the field (Kessler and Baldwin, 2004; Steppuhn et al., 2004; Frost et al., 2008) could be responsible for the equal performance of EV and irJAZh plants under natural conditions.

NaJAZh and Plant Development

As already introduced in this paper, jasmonate signaling regulates several non-defense-related plant responses. In *N. attenuata*, JAZh silencing had no visible effects on plant growth and/or development until elongation and the transition to flowering. Although flowers developed normally and seeds were produced as in wild-type plants, strongly silenced glasshouse-cultivated irJAZh plants developed visible necrotic lesions on their leaves (Fig. 9). This process resembled the PCD in plants that occurs during the hypersensitive response induced by pathogens; however, in irJAZh, it occurred spontaneously. PCD is closely associated with the accumulation of ROS in plant cells during the hypersensitive response (Allan and Fluhr, 1997; Desikan et al., 1998; Houot et al., 2001; Mittler et al., 2004; Cheeseman, 2007; Quan et al., 2008), which is known to inhibit the growth of biotrophic pathogens in plants. PCD also occurs in response to wounding, ozone and UV exposure, and cold and high-light stress (Pennell and Lamb, 1997; Buckner et al., 2000; Rao

et al., 2000a, 2000b; Beers and McDowell, 2001; Pasqualini et al., 2003). In addition, PCD is associated with plant growth and development; it occurs during senescence, pollen development, and vascular tissue differentiation (Wang et al., 1996; Pennell and Lamb, 1997; Calderon-Urrea and Dellaporta, 1999; Buckner et al., 2000; Wu and Cheun, 2000; Lee and Chen, 2002).

In our experiments, the *NaJAZh* gene appeared to be directly (or indirectly) responsible for the ectopic accumulation of H_2O_2 in *N. attenuata* leaves, which correlated with the elevated expression of several PCD marker genes in irJAZh plants. Previously, it has been shown that MeJA treatment induces ROS production in plants (Orozco-Cárdenas et al., 2001; Hung and Kao, 2007; Reinbothe et al., 2009), and it was shown that *Atrboh* (a respiratory burst oxidase homolog) D and F genes were required for COI1-dependent H_2O_2 production in Arabidopsis leaves treated with MeJA (Maruta et al., 2011). In particular, H_2O_2 accumulation was essential for the induction of JA-dependent genes such as *vegetative storage protein1* (*VSP1*) and Arabidopsis NAC domain-containing transcription factors *ANAC019* and *ANAC055*, suggesting that JA-controlled ROS is playing an active role as a secondary messenger in various physiological and defense-related processes in plants. Therefore, if NaJAZh works as an actual suppressor of ROS, some of the NaJAZh-silencing phenotypes could be attributed to the ectopic ROS accumulation that occurred even in the absence of JA in irJAZh plants.

From our data, we surmise that NaJAZh exerts a controlling function over the senescence process in mature tobacco leaves, possibly by controlling ROS levels in these leaves. A number of previous studies suggested that JA signaling intersects with senescence in plants (Weidhase et al., 1987; Parthier, 1990; He et al., 2002; Kong et al., 2006; Balbi and Devoto, 2008, Shan et al., 2011). Therefore, in the absence of a NaJAZh repressor, the leaves could enter a premature and/or exaggerated senescence process, as observed in irJAZh plants. However, the role of JA in the senescence process was recently questioned in the literature, by showing that JA-induced senescence differs from natural age-related senescence processes. Because none of the known JA signaling and biosynthetic mutants in Arabidopsis showed obvious senescence-related phenotypes (Schommer et al., 2008; Seltmann et al., 2010), additional research is required to understand the exact role of endogenous JAs and JAZ proteins in the regulation of this developmental process.

CONCLUSION

In this paper, we show that a single *JAZ* gene controls a suite of JA-dependent defense responses in a native tobacco (Fig. 12). Furthermore, our results point to a novel type of cross talk among individual JAZ proteins, which is demonstrated by the positive regulatory function of a NaJAZh repressor in nicotine accumulation in *N. attenuata* plants. Finally, a novel role for a JAZ protein in controlling ROS levels is demonstrated. However, despite current progress and the analysis of individual *JAZ* genes, much work is still required to fully understand the complex regulatory network of JAZ proteins. In particular, the identity of downstream TFs interacting with, and directly repressed by, JAZ repressors needs to be identified in order to connect JAZ proteins and downstream physiological responses occurring during stress exposure and/or development in plants.

MATERIALS AND METHODS

Plant Material and Growth Conditions

The 31st inbred generation of *Nicotiana attenuata* seeds (originally collected in Utah) was used for all experiments and the generation of transgenic plants. Seeds were germinated as described previously by Krügel et al. (2002), and approximately 10 d after germination, the seedlings were transferred into Teku plastic pots (Pöppelmann; http://www.poeppelmann.com) containing peat-based substrate (Tonsubstrat; Klasmann-Deilmann; http://www.klasmann-deilmann.com). The plantlets were maintained in the growth chamber under

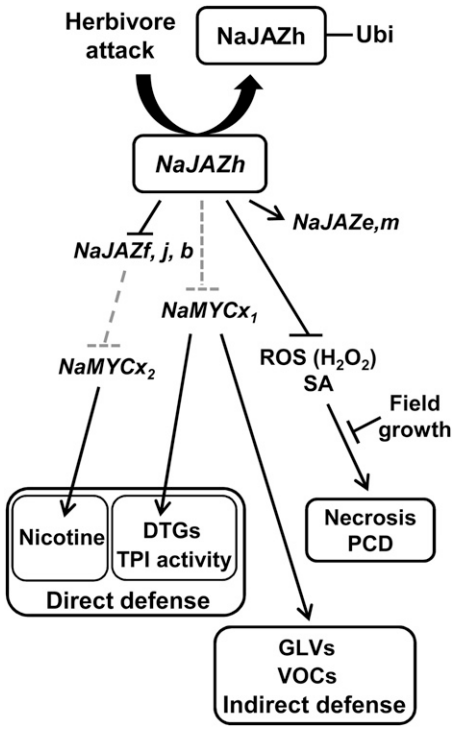

Figure 12. Summary of JAZh function in *N. attenuata* plants. NaJAZh is a major repressor of JA-dependent defense responses, including direct (DTGs and TPI activity) and indirect (GLVs and VOCs) defenses. It is proposed that NaJAZh regulates nicotine accumulation via interaction with other *JAZ* genes in *N. attenuata*. Furthermore, NaJAZh is required for direct or indirect repression of ROS, SA, and PCD during plant development in the glasshouse; necrosis (PCD) is prevented by an unknown environmental factor in the field. The black lines indicate interactions established in this paper; gray dashed lines show predicted components of the JAZ signaling pathways.

a 16-h-light/8-h-dark regime at 26°C. After an additional 10 to 12 d, the plants were transplanted into individual 1-L pots with the same substrate and maintained in the glasshouse (16 h of natural daylight supplemented by Philips Master Sun-T PIA Agro 400-W or 600-W sodium lights, temperature of 23°C–25°C, and 45%–55% relative humidity/8 h of dark, 19°C–23°C, 45%–55% relative humidity). The plants were supplied daily with water containing nutrients (0.5 g L^{-1} Peters Allrounder fertilizer [Scotts] containing nitrate, potassium, kalium, and magnesium + 0.1 g L^{-1} Borax; nutrient levels were adjusted weekly by checking the conductivity of the watering solution and resupplying nutrients) using an automatic glasshouse watering system. Unless stated otherwise, experiments were conducted with transient leaves (i.e. leaves undergoing the source-sink transition; node −1) of approximately 35-d-old rosette-stage *N. attenuata* plants.

The release of transgenic plants was carried under Animal and Plant Health Inspection Service notification 06-242-3r-a3, and the seeds were imported to the United States under permit number 10-004-105m. For field releases, we germinated the seeds on Gamborg's B5 medium as described previously; approximately 15 d after germination, the seedlings were transferred to prehydrated 50-mm peat pellets (Jiffy 703; http://www.jiffypot.com), and the seedlings were gradually adapted to the high light and low relative humidity of the habitat over a 2-week-period. Finally, preadapted rosette-stage plants were transplanted into a field plot and watered daily for approximately 2 weeks until the roots had established and the plants were able to grow without water supplementation.

Plant Transformation

To generate irJAZh plants, we cloned a 240-bp fragment of the *NaJAZh* gene (Supplemental Fig. S2A) as an inverted repeat into the pSOL8 transformation vector containing a hygromycin (*hptII*) resistance gene as selection maker (Supplemental Fig. S2B). *N. attenuata* plants were transformed using the LBA4404 strain of *Agrobacterium tumefaciens* and the transformation method described by Krügel et al. (2002). Homozygous transgenic lines were selected by screening of T2 generation seeds that showed hygromycin resistance, and T-DNA insertions were confirmed by Southern-blot hybridization using genomic DNA from selected lines and a ^{32}P-labeled PCR fragment of the *hptII* gene as hybridization probe (Supplemental Fig. S3). Real-time qPCR was used to select the best silenced single-insert-containing transgenic lines, irJAZh-264, irJAZh-267, and irJAZh-368, which were used in further experiments.

Cloning of *N. attenuata JAZ* Genes

To clone *N. attenuata JAZ* genes, we first searched public EST databases using two conserved ZIM and Jas motifs of *JAZ* genes known from other plant species, including Arabidopsis (*Arabidopsis thaliana*) and tobacco (*Nicotiana tabacum*), to obtain a pool of tobacco-specific JAZ-related EST sequences. The sequences were then assembled into putative tobacco *JAZ* genes using the publicly available CAP3 Sequence Assembly Program (http://deepc2.psi.iastate.edu/aat/cap/cap.html). Obtained assemblies were reblasted against the EST database to extend the initial JAZ sequences overlapping with Jas and ZIM domains. By repeating the process, we obtained 12 putative tobacco JAZ assemblies, presumably representing individual *JAZ* genes in tobacco, and designed 12 pairs of primers outside putative coding sequences to clone the corresponding full-length sequences from *N. attenuata*. Because the non-*N. attenuata* sequences were used for initial primer design (mainly *N. tabacum* and *Nicotiana benthamiana*), if necessary, the primers were redesigned until a clear PCR product of estimated length was amplified from the *N. attenuata* cDNA template in reverse transcription-PCR. Final and successful sets of primers are provided in Supplemental Table S3. In specific cases, a variation of the standard protocol was used; nine of the *N. attenuata JAZ* genes were cloned by direct PCR, whereas the three remaining genes (*JAZd*, *JAZl*, and *JAZm*) were cloned by the 3′ RACE method (3′ RACE System for RACE kit; Invitrogen). All genes were cloned from *N. attenuata* leaf cDNA samples, except for *NaJAZg*, which was only amplified when *N. attenuata* root cDNA was used. All 12 PCR products were cloned into pJET1.2/blunt Cloning Vector (Fermentas) using T4 ligase (Invitrogen) and transformed to *Escherichia coli* TOP10 electro-competent cells by a standard electroporation method. Plasmids containing the correct size of inserts were sequenced after isolating plasmids by the miniprep method (Nucleospin Extract II). At least three or more independent clones were fully sequenced for each type of insert.

Sequence Alignments and Construction of a Phylogenetic Tree

The translated putative protein full-length sequences of *NaJAZ* genes were aligned with other JAZ proteins using the ClustalW program, and a phylogenetic tree was built using bioinformatics software MEGA 5.05 (www.megasoftware.net) and the maximum likelihood bootstrap method (1,000 replicates).

Real-Time qPCR

Total RNA was extracted from approximately 100 mg of frozen leaf tissues with Trizol reagent as recommended by the manufacturer (Invitrogen). The RQ1 RNase-Free DNase was used to treat RNA following the manufacturer's instructions (Promega). The remaining DNase was removed by phenol extraction and precipitated with the addition of 3 M sodium acetate (pH 5.2) and pure ethanol. The cDNA was prepared from 1 μg of total RNA using RevertAid H Minus reverse transcriptase (Fermentas) and oligo(dT) primer (Fermentas). Real-time qPCR was conducted with synthesized cDNA using the core reagent kit for SYBR Green I (Eurogentec) and gene-specific primer pairs (Supplemental Tables S4 and S5) using Mx3005P PCR cycler (Stratagene). Relative gene expression was calculated from calibration curves obtained by an analysis of a dilution series of cDNA samples, and the values were normalized by the expression of the tobacco housekeeping gene *NtEF*α*1* (for *N. tabacum* elongation factor α-1). All reactions were performed using the following qPCR conditions: initial denaturation step of 95°C for 30 s, followed by 40 cycles each of 95°C for 30 s, 58°C for 30s, and 72°C for 1 min, followed by melting curve analysis of PCR products.

Herbivore Bioassays in the Glasshouse

Specialist herbivore *Manduca sexta* performance was conducted with the wild type and two independent irJAZh lines (irJAZh-267 and -368) during the 13-d time interval. Plants were grown in randomized spatial order on the same table in the glasshouse until the rosette stage (approximately 30 d after germination) or the elongated stage (close to flowering; approximately 40 d after germination). One freshly hatched *M. sexta* neonate was placed on the rosette leaf of each plant. The larval fresh mass was measured on days 5, 7, 9, 11, and 13 after initial feeding.

Phytohormone Analysis

Approximately 100 mg of frozen leaf material was homogenized with two steel balls in a Genogrider 2000 (SPEX Certi Prep) at 1,200 strokes min^{-1}, 30 s after freezing the samples and cooling plastic racks in liquid nitrogen. Phytohormones (JA, JA-Ile, SA, and ABA) were extracted by vortexing for 10 min after the addition of ethyl acetate spiked with internal standard: 200 ng of [$^2H_2$]JA and 40 ng each of JA-[$^{13}C_6$]Ile, [$^2H_4$]SA, and [$^2H_6$]ABA. The extracted samples were centrifuged at 16,100*g* at 4°C for 15 min, and the upper organic phases were transferred into clean tubes. Samples were evaporated to near dryness in a vacuum concentrator (Eppendorf) under reduced pressure. Hormone extracts were reconstituted in 500 μL of 70% (v/v) methanol:water for analysis with the Varian 1200 LC-ESI-MS/MS system as described by Gilardoni et al. (2011). The phytohormones were detected in negative ESI mode. Molecular ions $[M-H]^-$ at mass-to-charge ratio (*m/z*) 209, 322, 137, and 263 (213, 328, 141, and 269), generated from endogenous JA, JA-Ile, SA, and ABA (or their internal standards), were fragmented under 12-, 19-, 15- and 9-V collision energy, respectively. The ratios of ion intensities of the respective product ions and internal standards, *m/z* 59 and 63, *m/z* 130 and 136, *m/z* 93 and 97, and *m/z* 153 and 159, were used to quantify endogenous JA, JA-Ile, SA, and ABA, respectively. The resulting amounts of hormones were divided by the fresh mass of plant material used for the extraction of each sample.

Analysis of Secondary Metabolites by HPLC

The samples were extracted for a shared analysis of secondary metabolites by HPLC and individual DTGs by LC-ESI-MS/MS with the extraction method described by Heiling et al. (2010). Approximately 100 mg of frozen leaf material was homogenized with two steel balls by Genogrider 2000 (SPEX Certi Prep) at 1,200 strokes min^{-1}, 45 s, twice with 1 mL of buffer A (60% solution 1; 2.3 mL L^{-1} acetic acid, 3.41 g L^{-1} ammonium acetate adjusted to pH 4.8, 1 M

NH_4OH, and 40% [v/v] methanol) spiked with 120 ng of glycyrrhizinic acid as an internal standard for the determination of individual DTGs. Supernatants were collected after 20 min of centrifugation at 16,100*g* at 4°C. One microliter of particle-free supernatant (after additional centrifugation) was analyzed by HPLC (Agilent-HPLC 1100 series) using a chromatographic column (Chromolith FastGradient RP18e, 50 × 2 mm; Merck) connected to a precolumn (Gemini NX RP18, 3 μm, 2 × 4.6 mm; Phenomenex) with the column oven set at 40°C. Separated samples were detected with photodiode array and evaporative light-scattering detectors (Varian). The mobile phase, comprising solvent A (0.1% formic acid and 0.1% ammonium hydroxide solution in water [pH 3.5]) and solvent B (methanol), was used in a gradient mode (time/concentration [min/%] for A: 0:00/100, 0.50/100, 6.50/20, 10:00/20, 15:00/100) with a flow rate of 0.8 mL min^{-1}. Under these conditions, nicotine eluted at a retention time of 0.5 min (detected by UV A_{260}) and CP, chlorogenic acid (CGA), and DCS eluted at retention times of 2.6, 3.0, and 3.9 min, respectively (detected at 320 nm). Rutin eluted at a retention time of 4.7 min and was detected at 360 nm. The DTG peak pool eluting between retention times of 7.0 and 8.5 min was detected by evaporative light-scattering detection. The peak areas were integrated using Chromeleon chromatographic software (version 6.8; Dionex), and the amount of metabolites in plant tissue was calculated using an external dilution series of standard mixtures of nicotine, CGA, and rutin. CP and DCS contents were estimated based on the external CGA calibrations and expressed as CGA equivalents in the figures.

Analysis of Individual DTGs by the LC-ESI-MS/MS Method

Samples were prepared as described above for the secondary metabolite analysis by HPLC. Before analysis of individual DTGs, particle-free extracts were first diluted (1:50) with buffer B (10× diluted buffer A with 40% [v/v] methanol:water), and 10 μL of diluted extract was analyzed by the Varian 1200 LC-ESI-MS/MS system as described previously by Heiling et al. (2010).

TPI Activity Assay

Total protein fractions were extracted from approximately 100 mg of frozen leaf materials as described by Jongsma et al. (1994) with 300 μL of cold extraction buffer (0.1 M TRIS-HCl, pH 7.6, 5% polyvinylpolypyrrolidone, 2 mg mL^{-1} phenylthiourea, 5 mg mL^{-1} diethyldithiocarbamate, and 0.05 M Na_2EDTA). TPI activity in plant extracts was determined by the radial diffusion assay as described by Jongsma et al. (1993). Quantification of TPI activity in each sample was conducted using a standard soybean trypsin inhibitor (Sigma-Aldrich) calibration curve located on the same plate and normalized with total protein concentrations in each plant extract.

Volatile Collection and Analysis

A single leaf growing at node −1 was enclosed immediately after W+OS elicitation in a 50-mL plastic container connected to self-packed Porapak Q filters (20 mg of Porapak [Sigma-Aldrich] packed with silanized glass wool and Teflon tubing in the column bodies [Analytical Research Systems, Inc., Gainesville, FL] as described by Halitschke et al. [2000]). The ambient air was pulled from the trapping container through the tubing connected to the Porapak Q filter by pressurized air at 2 to 3 bar (using a Venturi aspirator able to create vacuum perpendicular to the direction of air flow). The air flow was adjusted to 200 to 300 mL min^{-1} with individual valves attached to a custom-made manifold, and the air flow of each outlet was kept constant over the entire trapping period of 24 h. After trapping, Porapak Q filters were stored at −20°C until elution of volatiles with 250 μL of dichloromethane spiked with 320 ng of tetraline internal standard (Sigma-Aldrich) into a gas chromatography vial containing a glass insert for small volume samples. The samples were analyzed by the CP-3800 GC Varian Saturn 4000 ion-trap mass spectrometer (Varian) connected to a nonpolar ZB5 column (30-m × 0.25-mm i.d., 0.25-μm film thickness; Phenomenex). One microliter of samples was injected by a CP-8400 autoinjector (Varian) onto the column in splitless mode; the injector was returned to a 1:70 split ratio 0.5 min after injection through the end of each run. The gas chromatograph was programmed as follows: injector held at 250°C, initial column temperature at 40°C held for 5 min, then ramped at 5°C min^{-1} to 185°C, finally at 30°C min^{-1} to 300°C, and held for 0.17 min. Helium carrier gas was used, and the column flow was set to 1 mL min^{-1}. Eluted compounds from the gas chromatograph column were transferred to a Varian Saturn 4000 ion-trap mass spectrometer for analysis. The mass spectrometer was programmed as follows: transfer line at 250°C, trap temperature of 110°C, ion source temperature of 200°C, manifold temperature of 50°C, and scan range from 40 to 300 *m/z* at 1.02 spectra s^{-1} as described by Schuman et al. (2009). Individual volatile compound peaks were quantified by peak areas using Mass Spectrometer Workstation software (Varian) and normalized by the peak area of the internal standard (tetraline) in each sample. The identification of compounds was conducted by gas chromatography, and retention times and mass spectra were compared with mass spectra database libraries, Wiley version 6 and the National Institute of Standards and Technology.

For volatile trapping in the field, we used single-use charcoal traps (ORBO-32 standard; Supelco) connected to self-made ozone scrubbers that contained eight-ply of 65-mm-diameter MnO_2-coated copper gauze to prevent the oxidation of terpenes and GLVs by ozone. A vacuum pump (DAA-V114-GB; Gast) powered by a car battery pulled air through the containers in the field. Treated plants were covered with open-ended transparent plastic cups to enhance the collection efficiency of released volatiles after elicitation of the leaves with W+OS (control plants remained untreated).

Microarray Analysis

Three biological replicates of node −1 leaves from wild-type and irJAZh-368 rosette-stage plants 2 h after elicitation with W+OS were used for the microarray analysis. Total RNA was extracted as described by Kistner and Matamoros (2005), and cDNA preparation and hybridization were performed as described by Kallenbach et al. (2011). Agilent platform GPL13527 (sample series GSE33681) deposited at the Gene Expression Omnibus (http://www.ncbi.nlm.nih.gov/geo/) was used for hybridizations. Raw microarray data were processed by SAM software version 3.11 (Significance Analysis of Microarrays; Stanford University; Tusher et al., 2001) after 75% percentile normalization and $\log_2$ transformation of the raw signal output values. Changes in gene expression were considered significant when fold changes (irJAZh versus the wild type) were larger than 3.0 or smaller than 0.33 and the false discovery rate was less than 4.82%.

H_2O_2 Measurements

H_2O_2 in the leaves was determined by semiquantitative DAB staining and by quantitative Amplex Red assays. For DAB staining, the leaves were incubated overnight in 1 mg mL^{-1} DAB solution in the dark at room temperature. To clear the stained leaves, we incubated them for 5 min in a 95°C water bath with a prewarmed lactic acid:glycerol:ethanol (1:1:3) mixture and repeated this procedure three to four times. The leaves were then transferred to a glycerol:ethanol (1:1) mixture and incubated overnight. H_2O_2 accumulation was determined as brown DAB precipitate on leaves.

For quantitative H_2O_2 measurements, we used the Amplex Red Hydrogen Peroxide/Peroxidase Assay Kit (Invitrogen). H_2O_2 was extracted from approximately 100 mg of liquid nitrogen-frozen leaf material that was stored under the same conditions. Liquid nitrogen-ground leaves were incubated on ice for 10 min after mixing with approximately 50 mg of activated charcoal and 200 μL of 25 mM HCl extraction buffer. The supernatants were transferred to clean tubes after 20 min of centrifugation at 16,100*g* and 4°C. The supernatants were used for H_2O_2 determination with the Amplex Red kit as follows: 5 μL of each sample was mixed with 45 μL of reaction buffer and 50 μL of working solution containing Amplex Red reagent and horseradish peroxidase on 96-well plates and incubated in the dark for 30 min. H_2O_2 content was determined from the amount of oxidized Amplex reagent with a TECAN Infinite M200 plate reader (Tecan) in fluorescence mode (excitation/emission = 530/590 nm. The concentrations of H_2O_2 in the samples were calculated from external H_2O_2 calibration curves measured on the same 96-well plate together with the samples.

Chlorophyll Measurements

Chlorophyll content was determined in wild-type and irJAZh plants that were supplied with or remained without extra nitrate (50 mL of 20 mM NH_4NO_3 every 2 d) from 34 to 50 d after germination using a chlorophyll meter (SPAD-502; Minolta). Averaged values of chlorophyll measured in three different areas of the leaf were calculated.

Field Bioassays

The field experiments were performed in the field plot at the Lytle Ranch Preserve, Utah. Fifteen pairs of EV and irJAZh plants were planted and grown in the field plot. One rosette leaf of each EV and irJAZh plant was treated with W+OS and harvested for the analysis of secondary metabolites, phytohormone, and gene expression at designated time intervals. Damage of plants by natural herbivores was determined by estimating the percentage of leaf area that was damaged by each herbivore relative to the total leaf area of the plant (Noctuidae larvae, *Spodoptera* spp.; flea beetles, *Epitrix* species; mirids, *Tupiocoris notatus*). A representative measurement conducted on June 2, 2011, is shown in Supplemental Figure S11.

Statistical Analysis

Data were analyzed with StatView 5.0 software (SAS Institute) using appropriate methods (e.g. Student's *t* test for pair comparisons and ANOVA followed by Fisher's protected least significant differences for multiple samples).

Accession numbers are as follows: NtEFα1, D63396; *Arabidopsis thaliana* JAZ (AtJAZ): AtJAZ1 (At1g19180), AtJAZ2 (At1g74950), AtJAZ3 (At3g17860), AtJAZ4 (At1g48500), AtJAZ5 (At1g17380), AtJAZ6 (At1g72450), AtJAZ7 (At2g34600), AtJAZ8 (At1g30135), AtJAZ9 (At1g70700), AtJAZ10 (At5g13220), AtJAZ11 (At3g43440), AtJAZ12 (At5g20900); *Oryza sativa* JAZ (OsJAZ): OsJAZ1 (AK061602), OsJAZ2 (AK073589), OsJAZ3 (AK070649), OsJAZ4 (AK120087), OsJAZ5 (AK061842), OsJAZ6 (AK065604), OsJAZ7 (AK108738), OsJAZ8 (AK065170), OsJAZ9 (AK103459), OsJAZ10 (AK059441), OsJAZ11 (AK107750), OsJAZ12 (AK107003); *Solanum lycopersicum* JAZ (SlJAZ): SlJAZ1 (Solyc07g042170), SlJAZ2 (Solyc12g009220), SlJAZ3 (Solyc03g122190), SlJAZ4 (Solyc12g049400), SlJAZ5 (Solyc03g118540), SlJAZ6 (Solyc01g005440), SlJAZ7 (Solyc11g011030), SlJAZ8 (Solyc06g068930), SlJAZ9 (Solyc08g036640), SlJAZ10 (Solyc08g036620), SlJAZ11 (Solyc08g036660), SlJAZ12 (Solyc01g009740); *Nicotiana tabacum* JAZ (NtJAZ): NtJAZ1 (AB433896), NtJAZ2 (AB433897), NtJAZ3 (AB433898); and *Nicotiana attenuata* JAZ (NaJAZ): NaJAZa (JQ172758), NaJAZb (JQ172759), NaJAZc.1 (JQ172760), NaJAZc.2 (JQ172761), NaJAZd (JQ172762), NaJAZe (JQ172763), NaJAZf (JQ172764), NaJAZg (JQ172765), NaJAZh (JQ172766), NaJAZj (JQ172767), NaJAZk.1 (JQ172768), NaJAZk.2 (JQ172769), NaJAZl (JQ172770), NaJAZm (JQ172771).

Supplemental Data

The following materials are available in the online version of this article.

Supplemental Figure S1. Differential splicing of *NaJAZ* genes.

Supplemental Figure S2. NaJAZh sequence and vector used for plant transformation.

Supplemental Figure S3. Southern blot and number of T-DNA insertions in genomes of stable transgenic irJAZh lines.

Supplemental Figure S4. Transcript levels of *NaJAZ* genes in irJAZh plants determined by microarrays.

Supplemental Figure S5. Nicotine levels and *NaPMT* gene expression in roots.

Supplemental Figure S6. Content of secondary metabolites in wild-type and irJAZh plants in the glasshouse.

Supplemental Figure S7. Secondary metabolite levels in *M. sexta*-fed leaves from wild-type and irJAZh plants in the glasshouse.

Supplemental Figure S8. Necrotic lesion symptoms of irJAZh plants were lost after crossing of homozygous irJAZh-267 with wild-type plants.

Supplemental Figure S9. Silencing efficiency of *NaJAZh* in field-grown EV and irJAZh plants.

Supplemental Figure S10. Secondary metabolite levels determined in field-grown plants.

Supplemental Figure S11. Individual DTGs determined in EV and NaJAZh-silenced plants grown in the native habitat in the Great Basin Desert.

Supplemental Figure S12. Volatile emission rates of EV and irJAZh plants grown in the native habitat in the Great Basin Desert.

Supplemental Figure S13. Herbivore damage inflicted by the native herbivore community to EV and NaJAZh-silenced plants grown in *N. attenuata*'s native habitat in the Great Basin Desert.

Supplemental Figure S14. DAB staining in the leaves from field-grown EV and irJAZh plants.

Supplemental Figure S15. Leaves of irJAZh and EV plants grown in the native habitat of the Great Basin Desert.

Supplemental Table S1. Up-regulated genes in irJAZh plants compared with wild-type plants by microarray.

Supplemental Table S2. Down-regulated genes in irJAZh plants compared with wild-type plants by microarray.

Supplemental Table S3. Primer sequences used for cloning of *JAZ* genes from *N. attenuata*.

Supplemental Table S4. Primer sequences used in real-time qPCR of *NaJAZ* genes.

Supplemental Table S5. Primer sequences used in real-time qPCR experiments.

Supplemental Text S1. Protein sequence alignment used to build the phylogenetic tree in Figure 1.

Supplemental Text S2. Nucleotide sequence alignment of *NaJAZ* genes that are regulated by silencing of *NaJAZh* against the sequence of an inverted repeat construct used in irJAZh plants.

ACKNOWLEDGMENTS

We thank Klaus Gase and Gustavo Bonaventure for help with the preparation of materials for microarrays; Wibke Kröber for hybridization of Agilent microarrays; Sang-Gyu Kim for providing plant materials for a time-course microarray experiment; Antje Wissgott for help with cloning of *NaJAZ* genes; Daniel Veit for constructing a custom-made manifold for volatile trapping; Danny Kessler, Celia Diezel, Meredith Schuman, Mario Kallenbach, and Mariana Stanton for helping with field experiments; Andreas Weber and Andreas Schünzel for growing the plants in the glasshouse; Brigham Young University for the use of its field station, the Lytle Ranch Preserve; and the Animal and Plant Health Inspection Service for constructive regulatory oversight of the field releases.

Received January 11, 2012; accepted April 5, 2012; published April 9, 2012.

LITERATURE CITED

Allan AC, Fluhr R (1997) Two distinct sources of elicited reactive oxygen species in tobacco epidermal cells. Plant Cell **9:** 1559–1572

Allmann S, Baldwin IT (2010) Insects betray themselves in nature to predators by rapid isomerization of green leaf volatiles. Science **329:** 1075–1078

Balbi V, Devoto A (2008) Jasmonate signalling network in *Arabidopsis thaliana*: crucial regulatory nodes and new physiological scenarios. New Phytol **177:** 301–318

Baldwin IT, Kessler A, Halitschke R (2002) Volatile signaling in plant-plant-herbivore interactions: what is real? Curr Opin Plant Biol **5:** 351–354

Baldwin IT, Zhang ZP, Diab N, Ohnmeiss TE, McCloud ES, Lynds GY, Schmelz EA (1997) Quantification, correlations and manipulations of wound-induced changes in jasmonic acid and nicotine in *Nicotiana sylvestris*. Planta **201:** 397–404

Beers EP, McDowell JM (2001) Regulation and execution of programmed cell death in response to pathogens, stress and developmental cues. Curr Opin Plant Biol **4:** 561–567

Boter M, Ruíz-Rivero O, Abdeen A, Prat S (2004) Conserved *MYC* transcription factors play a key role in jasmonate signaling both in tomato and *Arabidopsis*. Genes Dev **18:** 1577–1591

Browse J (2009) Jasmonate passes muster: a receptor and targets for the defense hormone. Annu Rev Plant Biol **60:** 183–205

Browse J, Howe GA (2008) New weapons and a rapid response against insect attack. Plant Physiol **146:** 832–838

Buckner B, Johal GS, Janick-Buckner D (2000) Cell death in maize. Physiol Plant **108:** 231–239

Calderon-Urrea A, Dellaporta SL (1999) Cell death and cell protection genes determine the fate of pistils in maize. Development **126:** 435–441

Cheeseman JM (2007) Hydrogen peroxide and plant stress: a challenging relationship. Plant Stress **1:** 4–15

Cheng Z, Sun L, Qi T, Zhang B, Peng W, Liu Y, Xie D (2011) The bHLH transcription factor MYC3 interacts with the jasmonate ZIM-domain proteins to mediate jasmonate response in *Arabidopsis*. Mol Plant **4:** 279–288

Chini A, Fonseca S, Chico JM, Fernández-Calvo P, Solano R (2009) The ZIM domain mediates homo- and heteromeric interactions between *Arabidopsis* JAZ proteins. Plant J **59:** 77–87

Chini A, Fonseca S, Fernández G, Adie B, Chico JM, Lorenzo O, García-Casado G, López-Vidriero I, Lozano FM, Ponce MR, et al (2007) The JAZ family of repressors is the missing link in jasmonate signalling. Nature **448:** 666–671

Chung HS, Cooke TF, Depew CL, Patel LC, Ogawa N, Kobayashi Y, Howe GA (2010) Alternative splicing expands the repertoire of dominant JAZ repressors of jasmonate signaling. Plant J **63:** 613–622

Chung HS, Howe GA (2009) A critical role for the TIFY motif in repression of jasmonate signaling by a stabilized splice variant of the JASMONATE ZIM-domain protein JAZ10 in *Arabidopsis*. Plant Cell **21:** 131–145

Chung HS, Koo AJ, Gao X, Jayanty S, Thines B, Jones AD, Howe GA (2008) Regulation and function of Arabidopsis JASMONATE ZIM-domain genes in response to wounding and herbivory. Plant Physiol **146:** 952–964

Chung HS, Niu Y, Browse J, Howe GA (2009) Top hits in contemporary JAZ: an update on jasmonate signaling. Phytochemistry **70:** 1547–1559

Cipollini DF, Bergelson J (2001) Plant density and nutrient availability constrain constitutive and wound-induced expression of trypsin inhibitors in *Brassica napus*. J Chem Ecol **27:** 593–610

Cipollini DF, Purrington CB, Bergelson J (2003) Costs of induced responses in plants. Basic Appl Ecol **4:** 79–89

Demianski AJ, Chung KM, Kunkel BN (2012) Analysis of Arabidopsis *JAZ* gene expression during *Pseudomonas syringae* pathogenesis. Mol Plant Pathol **13:** 46–57

Desikan R, Reynolds A, Hancock JT, Neill SJ (1998) Harpin and hydrogen peroxide both initiate programmed cell death but have differential effects on defence gene expression in Arabidopsis suspension cultures. Biochem J **330:** 115–120

Devoto A, Ellis C, Magusin A, Chang H-S, Chilcott C, Zhu T, Turner JG (2005) Expression profiling reveals COI1 to be a key regulator of genes involved in wound- and methyl jasmonate-induced secondary metabolism, defence, and hormone interactions. Plant Mol Biol **58:** 497–513

Devoto A, Nieto-Rostro M, Xie D, Ellis C, Harmston R, Patrick E, Davis J, Sherratt L, Coleman M, Turner JG (2002) COI1 links jasmonate signalling and fertility to the SCF ubiquitin-ligase complex in Arabidopsis. Plant J **32:** 457–466

Farmer EE, Alméras E, Krishnamurthy V (2003) Jasmonates and related oxylipins in plant responses to pathogenesis and herbivory. Curr Opin Plant Biol **6:** 372–378

Fernández-Calvo P, Chini A, Fernández-Barbero G, Chico J-M, Gimenez-Ibanez S, Geerinck J, Eeckhout D, Schweizer F, Godoy M, Franco-Zorrilla JM, et al (2011) The *Arabidopsis* bHLH transcription factors *MYC3* and *MYC4* are targets of JAZ repressors and act additively with *MYC2* in the activation of jasmonate responses. Plant Cell **23:** 701–715

Feys BJF, Benedetti CE, Penfold CN, Turner JG (1994) *Arabidopsis* mutants selected for resistance to the phytotoxin coronatine are male sterile, insensitive to methyl jasmonate, and resistant to a bacterial pathogen. Plant Cell **6:** 751–759

Fonseca S, Chini A, Hamberg M, Adie B, Porzel A, Kramell R, Miersch O, Wasternack C, Solano R (2009) (+)-7-Iso-jasmonoyl-L-isoleucine is the endogenous bioactive jasmonate. Nat Chem Biol **5:** 344–350

Frost CJ, Mescher MC, Carlson JE, De Moraes CM (2008) Plant defense priming against herbivores: getting ready for a different battle. Plant Physiol **146:** 818–824

Gilardoni PA, Hettenhausen C, Baldwin IT, Bonaventure G (2011) *Nicotiana attenuata LECTIN RECEPTOR KINASE1* suppresses the insect-mediated inhibition of induced defense responses during *Manduca sexta* herbivory. Plant Cell **23:** 3512–3532

Glauser G, Grata E, Dubugnon L, Rudaz S, Farmer EE, Wolfender J-L (2008) Spatial and temporal dynamics of jasmonate synthesis and accumulation in *Arabidopsis* in response to wounding. J Biol Chem **283:** 16400–16407

Glazebrook J (2005) Contrasting mechanisms of defense against biotrophic and necrotrophic pathogens. Annu Rev Phytopathol **43:** 205–227

Grunewald W, Vanholme B, Pauwels L, Plovie E, Inzé D, Gheysen G, Goossens A (2009) Expression of the Arabidopsis jasmonate signalling repressor JAZ1/TIFY10A is stimulated by auxin. EMBO Rep **10:** 923–928

Habib H, Fazili KM (2007) Plant protease inhibitors: a defense strategy in plants. Biotechnol Mol Biol Rev **2:** 068–085

Halitschke R, Keßler A, Kahl J, Lorenz A, Baldwin IT (2000) Ecophysiological comparison of direct and indirect defenses in *Nicotiana attenuata*. Oecologia **124:** 408–417

Hara-Nishimura I, Hatsugai N, Nakaune S, Kuroyanagi M, Nishimura M (2005) Vacuolar processing enzyme: an executor of plant cell death. Curr Opin Plant Biol **8:** 404–408

Hartl M, Giri AP, Kaur H, Baldwin IT (2010) Serine protease inhibitors specifically defend *Solanum nigrum* against generalist herbivores but do not influence plant growth and development. Plant Cell **22:** 4158–4175

Hasegawa S, Sogabe Y, Asano T, Nakagawa T, Nakamura H, Kodama H, Ohta H, Yamaguchi K, Mueller MJ, Nishiuchi T (2011) Gene expression analysis of wounding-induced root-to-shoot communication in *Arabidopsis thaliana*. Plant Cell Environ **34:** 705–716

Hatsugai N, Kuroyanagi M, Yamada K, Meshi T, Tsuda S, Kondo M, Nishimura M, Hara-Nishimura I (2004) A plant vacuolar protease, VPE, mediates virus-induced hypersensitive cell death. Science **305:** 855–858

He Y, Fukushige H, Hildebrand DF, Gan S (2002) Evidence supporting a role of jasmonic acid in Arabidopsis leaf senescence. Plant Physiol **128:** 876–884

Heiling S, Schuman MC, Schoettner M, Mukerjee P, Berger B, Schneider B, Jassbi AR, Baldwin IT (2010) Jasmonate and ppHsystemin regulate key malonylation steps in the biosynthesis of 17-hydroxygeranyllinalool diterpene glycosides, an abundant and effective direct defense against herbivores in *Nicotiana attenuata*. Plant Cell **22:** 273–292

Houot V, Etienne P, Petitot AS, Barbier S, Blein JP, Suty L (2001) Hydrogen peroxide induces programmed cell death features in cultured tobacco BY-2 cells, in a dose-dependent manner. J Exp Bot **52:** 1721–1730

Howe GA, Jander G (2008) Plant immunity to insect herbivores. Annu Rev Plant Biol **59:** 41–66

Hung KT, Kao CH (2007) The participation of hydrogen peroxide in methyl jasmonate-induced NH_4^+ accumulation in rice leaves. J Plant Physiol **164:** 1469–1479

Jassbi AR, Gase K, Hettenhausen C, Schmidt A, Baldwin IT (2008) Silencing geranylgeranyl diphosphate synthase in *Nicotiana attenuata* dramatically impairs resistance to tobacco hornworm. Plant Physiol **146:** 974–986

Jongsma MA, Bakker PL, Peters J, Bosch D, Stiekema WJ (1995) Adaptation of *Spodoptera exigua* larvae to plant proteinase inhibitors by induction of gut proteinase activity insensitive to inhibition. Proc Natl Acad Sci USA **92:** 8041–8045

Jongsma MA, Bakker PL, Stiekema WJ (1993) Quantitative determination of serine proteinase inhibitor activity using a radial diffusion assay. Anal Biochem **212:** 79–84

Jongsma MA, Bakker PL, Visser B, Stiekema WJ (1994) Trypsin inhibitor activity in mature tobacco and tomato plants is mainly induced locally in response to insect attack, wounding and virus infection. Planta **195:** 29–35

Kallenbach M, Gilardoni PA, Allmann S, Baldwin IT, Bonaventure G (2011) C12 derivatives of the hydroperoxide lyase pathway are produced by product recycling through lipoxygenase-2 in *Nicotiana attenuata* leaves. New Phytol **191:** 1054–1068

Katsir L, Schilmiller AL, Staswick PE, He SY, Howe GA (2008) COI1 is a critical component of a receptor for jasmonate and the bacterial virulence factor coronatine. Proc Natl Acad Sci USA **105:** 7100–7105

Kaur H, Heinzel N, Schöttner M, Baldwin IT, Gális I (2010) R2R3-NaMYB8 regulates the accumulation of phenylpropanoid-polyamine conjugates, which are essential for local and systemic defense against insect herbivores in *Nicotiana attenuata*. Plant Physiol **152:** 1731–1747

Kessler A, Baldwin IT (2001) Defensive function of herbivore-induced plant volatile emissions in nature. Science **291:** 2141–2144

Kessler A, Baldwin IT (2004) Herbivore-induced plant vaccination. Part I. The orchestration of plant defenses in nature and their fitness consequences in the wild tobacco *Nicotiana attenuata*. Plant J **38:** 639–649

Kim S-G, Yon F, Gaquerel E, Gulati J, Baldwin IT (2011) Tissue specific diurnal rhythms of metabolites and their regulation during herbivore attack in a native tobacco, *Nicotiana attenuata*. PLoS ONE **6:** e26214

Kistner C, Matamoros M (2005) RNA isolation using phase extraction and LiCl precipitation. *In* AJ Márquez, ed, *Lotus japonicus* Handbook. Springer, Dordrecht, The Netherlands, pp 123–124

Koiwa H, Bressan RA, Hasegawa PM (1997) Regulation of protease inhibitors and plant defense. Trends Plant Sci **2:** 379–384

Kong Z, Li M, Yang W, Xu W, Xue Y (2006) A novel nuclear-localized CCCH-type zinc finger protein, OsDOS, is involved in delaying leaf senescence in rice. Plant Physiol **141:** 1376–1388

Koo AJ, Gao X, Jones AD, Howe GA (2009) A rapid wound signal activates the systemic synthesis of bioactive jasmonates in *Arabidopsis*. Plant J **59:** 974–986

Krügel T, Lim M, Gase K, Halitschke R, Baldwin IT (2002) *Agrobacterium*-mediated transformation of *Nicotiana attenuata*, a model ecological expression system. Chemoecology **12:** 177–183

Lee R-H, Chen S-CG (2002) Programmed cell death during rice leaf senescence is nonapoptotic. New Phytol **155:** 25–32

Li L, Zhao Y, McCaig BC, Wingerd BA, Wang J, Whalon ME, Pichersky E, Howe GA (2004) The tomato homolog of CORONATINE-INSENSITIVE1 is required for the maternal control of seed maturation, jasmonate-signaled defense responses, and glandular trichome development. Plant Cell **16:** 126–143

Lorenzo O, Chico JM, Sánchez-Serrano JJ, Solano R (2004) JASMONATE-INSENSITIVE1 encodes a *MYC* transcription factor essential to discriminate between different jasmonate-regulated defense responses in *Arabidopsis*. Plant Cell **16:** 1938–1950

Mandaokar A, Thines B, Shin B, Lange BM, Choi G, Koo YJ, Yoo YJ, Choi YD, Choi G, Browse J (2006) Transcriptional regulators of stamen development in *Arabidopsis* identified by transcriptional profiling. Plant J **46:** 984–1008

Maruta T, Inoue T, Tamoi M, Yabuta Y, Yoshimura K, Ishikawa T, Shigeoka S (2011) *Arabidopsis* NADPH oxidases, AtrbohD and AtrbohF, are essential for jasmonic acid-induced expression of genes regulated by *MYC2* transcription factor. Plant Sci **180:** 655–660

Melotto M, Mecey C, Niu Y, Chung HS, Katsir L, Yao J, Zeng W, Thines B, Staswick P, Browse J, et al (2008) A critical role of two positively charged amino acids in the Jas motif of *Arabidopsis* JAZ proteins in mediating coronatine- and jasmonoyl isoleucine-dependent interactions with the COI1 F-box protein. Plant J **55:** 979–988

Mewis I, Tokuhisa JG, Schultz JC, Appel HM, Ulrichs C, Gershenzon J (2006) Gene expression and glucosinolate accumulation in *Arabidopsis thaliana* in response to generalist and specialist herbivores of different feeding guilds and the role of defense signaling pathways. Phytochemistry **67:** 2450–2462

Mittler R, Vanderauwera S, Gollery M, Van Breusegem F (2004) Reactive oxygen gene network of plants. Trends Plant Sci **9:** 490–498

Niu Y, Figueroa P, Browse J (2011) Characterization of JAZ-interacting bHLH transcription factors that regulate jasmonate responses in *Arabidopsis*. J Exp Bot **62:** 2143–2154

Orozco-Cárdenas ML, Narváez-Vásquez J, Ryan CA (2001) Hydrogen peroxide acts as a second messenger for the induction of defense genes in tomato plants in response to wounding, systemin, and methyl jasmonate. Plant Cell **13:** 179–191

Parthier B (1990) Jasmonates: hormonal regulators or stress factors in leaf senescence? J Plant Growth Regul **9:** 57–63

Paschold A, Bonaventure G, Kant MR, Baldwin IT (2008) Jasmonate perception regulates jasmonate biosynthesis and JA-Ile metabolism: the case of COI1 in *Nicotiana attenuata*. Plant Cell Physiol **49:** 1165–1175

Paschold A, Halitschke R, Baldwin IT (2006) Using 'mute' plants to translate volatile signals. Plant J **45:** 275–291

Pasqualini S, Piccioni C, Reale L, Ederli L, Della Torre G, Ferranti F (2003) Ozone-induced cell death in tobacco cultivar Bel W3 plants: the role of programmed cell death in lesion formation. Plant Physiol **133:** 1122–1134

Pauwels L, Barbero GF, Geerinck J, Tilleman S, Grunewald W, Pérez AC, Chico JM, Bossche RV, Sewell J, Gil E, et al (2010) NINJA connects the co-repressor TOPLESS to jasmonate signalling. Nature **464:** 788–791

Pauwels L, Goossens A (2011) The JAZ proteins: a crucial interface in the jasmonate signaling cascade. Plant Cell **23:** 3089–3100

Pennell RI, Lamb C (1997) Programmed cell death in plants. Plant Cell **9:** 1157–1168

Qi T, Song S, Ren Q, Wu D, Huang H, Chen Y, Fan M, Peng W, Ren C, Xie D (2011) The jasmonate-ZIM-domain proteins interact with the WD-repeat/bHLH/MYB complexes to regulate jasmonate-mediated anthocyanin accumulation and trichome initiation in *Arabidopsis thaliana*. Plant Cell **23:** 1795–1814

Quan LJ, Zhang B, Shi WW, Li HY (2008) Hydrogen peroxide in plants: a versatile molecule of the reactive oxygen species network. J Integr Plant Biol **50:** 2–18

Rao MV, Koch JR, Davis KR (2000a) Ozone: a tool for probing programmed cell death in plants. Plant Mol Biol **44:** 345–358

Rao MV, Lee H-i, Creelman RA, Mullet JE, Davis KR (2000b) Jasmonic acid signaling modulates ozone-induced hypersensitive cell death. Plant Cell **12:** 1633–1646

Rask L, Andréasson E, Ekbom B, Eriksson S, Pontoppidan B, Meijer J (2000) Myrosinase: gene family evolution and herbivore defense in Brassicaceae. Plant Mol Biol **42:** 93–113

Reinbothe C, Springer A, Samol I, Reinbothe S (2009) Plant oxylipins: role of jasmonic acid during programmed cell death, defence and leaf senescence. FEBS J **276:** 4666–4681

Schaller A, Stintzi A (2009) Enzymes in jasmonate biosynthesis: structure, function, regulation. Phytochemistry **70:** 1532–1538

Schommer C, Palatnik JF, Aggarwal P, Chételat A, Cubas P, Farmer EE, Nath U, Weigel D (2008) Control of jasmonate biosynthesis and senescence by miR319 targets. PLoS Biol **6:** e230

Schuman MC, Heinzel N, Gaquerel E, Svatos A, Baldwin IT (2009) Polymorphism in jasmonate signaling partially accounts for the variety of volatiles produced by *Nicotiana attenuata* plants in a native population. New Phytol **183:** 1134–1148

Seltmann MA, Stingl NE, Lautenschlaeger JK, Krischke M, Mueller MJ, Berger S (2010) Differential impact of lipoxygenase 2 and jasmonates on natural and stress-induced senescence in Arabidopsis. Plant Physiol **152:** 1940–1950

Seo J-S, Joo J, Kim M-J, Kim Y-K, Nahm BH, Song SI, Cheong J-J, Lee JS, Kim J-K, Choi YD (2011) OsbHLH148, a basic helix-loop-helix protein, interacts with OsJAZ proteins in a jasmonate signaling pathway leading to drought tolerance in rice. Plant J **65:** 907–921

Shan X, Wang J, Chua L, Jiang D, Peng W, Xie D (2011) The role of Arabidopsis Rubisco activase in jasmonate-induced leaf senescence. Plant Physiol **155:** 751–764

Shan X, Zhang Y, Peng W, Wang Z, Xie D (2009) Molecular mechanism for jasmonate-induction of anthocyanin accumulation in *Arabidopsis*. J Exp Bot **60:** 3849–3860

Sheard LB, Tan X, Mao H, Withers J, Ben-Nissan G, Hinds TR, Kobayashi Y, Hsu FF, Sharon M, Browse J, et al (2010) Jasmonate perception by inositol-phosphate-potentiated COI1-JAZ co-receptor. Nature **468:** 400–405

Shikata M, Matsuda Y, Ando K, Nishii A, Takemura M, Yokota A, Kohchi T (2004) Characterization of *Arabidopsis* ZIM, a member of a novel plant-specific GATA factor gene family. J Exp Bot **55:** 631–639

Shoji T, Hashimoto T (2011) Tobacco MYC2 regulates jasmonate-inducible nicotine biosynthesis genes directly and by way of the NIC2-locus ERF genes. Plant Cell Physiol **52:** 1117–1130

Shoji T, Kajikawa M, Hashimoto T (2010) Clustered transcription factor genes regulate nicotine biosynthesis in tobacco. Plant Cell **22:** 3390–3409

Shoji T, Ogawa T, Hashimoto T (2008) Jasmonate-induced nicotine formation in tobacco is mediated by tobacco COI1 and JAZ genes. Plant Cell Physiol **49:** 1003–1012

Shoji T, Yamada Y, Hashimoto T (2000) Jasmonate induction of putrescine N-methyltransferase genes in the root of *Nicotiana sylvestris*. Plant Cell Physiol **41:** 831–839

Shroff R, Vergara F, Muck A, Svatoš A, Gershenzon J (2008) Nonuniform distribution of glucosinolates in *Arabidopsis thaliana* leaves has important consequences for plant defense. Proc Natl Acad Sci USA **105:** 6196–6201

Shyu C, Figueroa P, DePew CL, Cooke TF, Sheard LB, Moreno JE, Katsir L, Zheng N, Browse J, Howe GA (2012) JAZ8 lacks a canonical degron and has an EAR motif that mediates transcriptional repression of jasmonate responses in *Arabidopsis*. Plant Cell **24:** 536–550

Sogabe Y, Nakamura H, Nakagawa T, Hasegawa S, Asano T, Ohta H, Yamaguchi K, Mueller MJ, Kodama H, Nishiuchi T (2011) Visualization of wounding-induced root-to-shoot communication in *Arabidopsis*. Plant Signal Behav **6:** 1037–1039

Song S, Qi T, Huang H, Ren Q, Wu D, Chang C, Peng W, Liu Y, Peng J, Xie D (2011) The jasmonate-ZIM domain proteins interact with the

R2R3-MYB transcription factors *MYB21* and *MYB24* to affect jasmonate-regulated stamen development in *Arabidopsis*. Plant Cell **23:** 1000–1013

Steppuhn A, Gase K, Krock B, Halitschke R, Baldwin IT (2004) Nicotine's defensive function in nature. PLoS Biol **2:** E217

Strauss SY, Rudgers JA, Lau JA, Irwin RE (2002) Direct and ecological costs of resistance to herbivory. Trends Ecol Evol **17:** 278–285

Sun JQ, Jiang HL, Li CY (2011) Systemin/jasmonate-mediated systemic defense signaling in tomato. Mol Plant **4:** 607–615

Thines B, Katsir L, Melotto M, Niu Y, Mandaokar A, Liu G, Nomura K, He SY, Howe GA, Browse J (2007) JAZ repressor proteins are targets of the SCF(COI1) complex during jasmonate signalling. Nature **448:** 661–665

Tusher VG, Tibshirani R, Chu G (2001) Significance analysis of microarrays applied to the ionizing radiation response. Proc Natl Acad Sci USA **98:** 5116–5121

Vanholme B, Grunewald W, Bateman A, Kohchi T, Gheysen G (2007) The tify family previously known as ZIM. Trends Plant Sci **12:** 239–244

Wang H, Wu HM, Cheung AY (1996) Pollination induces mRNA poly(A) tail-shortening and cell deterioration in flower transmitting tissue. Plant J **9:** 715–727

Wasternack C (2007) Jasmonates: an update on biosynthesis, signal transduction and action in plant stress response, growth and development. Ann Bot (Lond) **100:** 681–697

Weidhase RA, Kramell H-M, Lehmann J, Liebisch H-W, Lerbs W, Parthier B (1987) Methyl-jasmonate-induced changes in the polypeptide pattern of senescing barley leaf segments. Plant Sci **51:** 177–186

Wink M, Roberts MF (1998) Compartmentation of alkaloid synthesis, transport, and storage. *In* M Wink, MF Roberts, eds, Alkaloids. Plenum Press, New York, pp 239–262

Wu HM, Cheun AY (2000) Programmed cell death in plant reproduction. Plant Mol Biol **44:** 267–281

Wu J, Baldwin IT (2010) New insights into plant responses to the attack from insect herbivores. Annu Rev Genet **44:** 1–24

Xie D-X, Feys BF, James S, Nieto-Rostro M, Turner JG (1998) COI1: an *Arabidopsis* gene required for jasmonate-regulated defense and fertility. Science **280:** 1091–1094

Yan J, Zhang C, Gu M, Bai Z, Zhang W, Qi T, Cheng Z, Peng W, Luo H, Nan F, et al (2009) The *Arabidopsis* CORONATINE INSENSITIVE1 protein is a jasmonate receptor. Plant Cell **21:** 2220–2236

Yan Y, Stolz S, Chételat A, Reymond P, Pagni M, Dubugnon L, Farmer EE (2007) A downstream mediator in the growth repression limb of the jasmonate pathway. Plant Cell **19:** 2470–2483

Zavala JA, Patankar AG, Gase K, Baldwin IT (2004b) Constitutive and inducible trypsin proteinase inhibitor production incurs large fitness costs in *Nicotiana attenuata*. Proc Natl Acad Sci USA **101:** 1607–1612

Zavala JA, Patankar AG, Gase K, Hui D, Baldwin IT (2004a) Manipulation of endogenous trypsin proteinase inhibitor production in *Nicotiana attenuata* demonstrates their function as antiherbivore defenses. Plant Physiol **134:** 1181–1190

Zhang H-B, Bokowiec MT, Rushton PJ, Han S-C, Timko MP (2012) Tobacco transcription factors *NtMYC2a* and *NtMYC2b* form nuclear complexes with the NtJAZ1 repressor and regulate multiple jasmonate-inducible steps in nicotine biosynthesis. Mol Plant **5:** 73–84